RAFFLES BULLETIN OF ZOOLOGY **74**: 360–382
Date of publication: 13 May 2026
DOI: 10.26107/RBZ-2026-0025
https://zoobank.org/urn:lsid:zoobank.org:pub:2F426397-2A36-4A45-8F2A-E28F54BCA59D

Quaternary fossil catfishes (Ariidae and Plotosidae) from the Rajang River Delta of Borneo

Ilman **Haziq**[1], László **Kocsis**[2*], Masatoshi **Sone**[3], Márton **Rabi**[4] & Adibah **Johari**[1]

Abstract. The island of Borneo, situated within the Indo-Australian Archipelago, is recognised as hosting the highest marine biodiversity on Earth today. However, the evolutionary history of fish biodiversity in this region remains poorly understood due to a sparse fossil record and a paucity of detailed taxonomic studies. This study presents the first fossil fauna of Siluriformes from Sarawak (Malaysian Borneo), comprising sea catfish (Ariidae) and eeltail catfish (Plotosidae). The material forms part of a Pleistocene/Holocene vertebrate fossil assemblage, which has been reworked and redeposited along the beach, recently discovered on Bruit Island in the Rajang River Delta. The assemblage comprises a mix of aquatic (e.g., bony fish, sharks) and nonaquatic (terrestrial mammals) fauna, with fish remains predominating, particularly the ariid catfishes, which represent the most common ray-finned fish fossils at the site. To facilitate the identification of the catfish fossils, we collected 13 extant ariid and plotosid species from Brunei and Sarawak and prepared their skeletal specimens for anatomical comparison, with a primary focus on skull allometry. The fossil material encompasses over 200 bones, including numerous cranial elements along with postcranial bones such as pectoral and dorsal spines, as well as vertebrae. Additionally, several fossilised ariid otoliths (lapilli) were recovered. Our taxonomic identification of these fossils indicates the presence of at least four ariid species: *Hexanematichthys sagor*, which was the most abundant, followed by *Plicofollis nella*, *Kyataphisa nenga*, and *Arius* cf. *maculatus*, and one plotosid species, *Plotosus* cf. *canius*. The habitat of the fossil catfish fauna from Sarawak is best attributed to a coastal marine and estuarine palaeoenvironment, analogous to modern transitional environments, such as the Rajang River Delta.

Key words. bone, otolith, allometry, sea catfish, Sarawak, Malaysia

INTRODUCTION

Ariidae (sea catfish) is one of the extant families within the order Siluriformes (catfish), comprising approximately 160 species across 40 living genera worldwide (Marceniuk et al., 2024; Froese & Pauly, 2025). These fish primarily inhabit marine coastal waters and estuaries in tropical and warm temperate regions, although many species migrate into or reside in freshwater and brackish-water environments (Nelson et al., 2016; Marceniuk et al., 2024). Ariidae is a well-defined monophyletic group supported by both morphological (Kailola, 2004; Diogo, 2005; Acero & Betancur-R, 2007; Marceniuk & Menezes, 2007, 2012) and molecular evidence (e.g., Sullivan et al., 2006; Betancur-R et al., 2007; Betancur-R, 2009).

Key anatomical synapomorphies of ariids include a large, well-developed lapillus otolith; an expanded otic capsule with associated bones (prootic, pterotic, exoccipital, and epioccipital); and a pronounced ventral process of the basioccipital (Acero & Betancur-R, 2007). Additionally, many sea catfish can be distinguished by the development of a fossa in the neurocranium, located between the articulations of the posttemporo-supracleithrum, extrascapular, and pterotic bones, features that contrast with those of most freshwater catfish (see Acero & Betancur, 2007; Aguilera et al., 2013). Note that recent discussion on siluriform cranial bone homologies proposes an alternative origin for some of these bones, where the posttemporal-supracleithrum represents the supracleithrum and the extrascapular refers to the posttemporal (Kubicek, 2022). Nevertheless, based on osteological features of the cranium, ariids are readily identifiable (Arratia, 2003), making these bones particularly useful for identifying fossil remains at the genus level, and in some cases, even at the species level (Aguilera et al., 2013, 2020).

In the fossil record, ariids are primarily represented by their characteristic lapillus otoliths, although cranial and post-cranial bones have also been described (Gayet & Meunier,

Accepted by: Kevin W. Conway

[1]Geology Group, Faculty of Science, Universiti Brunei Darussalam, Jalan Tungku Link, Gadong BE1410, Brunei Darussalam

[2]Institute of Earth Surface Dynamics, University of Lausanne, Rue de la Mouline, 1015 Lausanne, Switzerland, Email: laszlo.kocsis@unil.ch (*corresponding author)

[3]Department of Geology, Faculty of Science, University of Malaya, 50603 Kuala Lumpur, Malaysia

[4]Institute of Geosciences, University of Tübingen, Hölderlinstraße 12, 72074 Tübingen, Germany

ISSN 2345-7600 (electronic) | ISSN 0217-2445 (print)

2003; Ferraris, 2007). Numerous fossil species have been erected based on dorsal and pectoral spines, but some may require future revision to confirm their validity (Ferraris, 2007). The New World fossil record of ariids, especially Neogene material from South America, is among the best studied (e.g., Aguilera et al., 2013, 2020), while some of the oldest likely ariid otoliths are derived from Late Cretaceous deposits in North America (Frizzell, 1965; Huddleston & Savoie, 1983). In Africa, ariid fossils are known from Egypt. First, *Arius frassi* Peyer, 1928 was described from the middle Eocene Mokattam Formation. Second, it was also reported from the late Eocene Birket Qarun Formation (El-Sayed et al., 2020), where another ariid species, *Qarmoutus hitanensis* El-Sayed et al., 2017, was described based on cranial and associated body parts. In Asia, the Eocene species, *Arius kutchensis* Rao, 1956, has been known from West India, primarily based on skull remains (see also Sahni & Mishra, 1975). This is the most detailed record of ariid fossils from the Indo-Pacific region, where otherwise only sporadic bone fragments and otoliths have been documented.

Here, we present, for the first time, a rich catfish fossil assemblage from Borneo, based on numerous bones found along the beach of Bruit Island in the Rajang River Delta, central Sarawak, East Malaysia. The site yielded a diverse, mixed vertebrate fauna, including remains of various fishes, reptiles, and both marine and terrestrial mammals. The mixed nature of the assemblage, along with the absence of in-situ stratigraphic beds, makes it difficult to determine the exact age of the fossils. To date, no source deposits have been identified in the hinterland of central Sarawak that could account for these fossils. The surrounding bedrock is thought to be of a Miocene–Pliocene age or older (e.g., Hutchison, 2005). This region is characterised by recent deltaic sedimentation and the extensive alluvial environment of the Rajang River and its tributaries (Fig. 1). Based on the overall composition of the aquatic fauna, some fossils are likely of marine origin from the South China Sea, while others are associated with the brackish or freshwater conditions of the Rajang River Delta. Most terrestrial remains were likely reworked from terrace deposits and/or transported from the delta plain via the Rajang River. Based on some terrestrial mammal teeth, the fossil assemblage is presumed to date to the Pleistocene or Holocene.

Southeast Asia is recognised as a region of exceptional marine biodiversity, hosting the highest diversity of marine fishes on Earth today (e.g., Cowman, 2014). Studying the fossil records from this region can provide important insights into the evolutionary history of this biodiversity. The most common modern ariids of the region are listed in Kailola (1999). Based on recent classifications, members of the tribe Ariini and subtribe Ariina, encompassing approximately 43 species in 17 genera, are present in Southeast Asia (Marceniuk et al., 2024; Froese & Pauly, 2025). In terms of fossil records, ariid otoliths have been reported from Sumatra (Frost, 1925), Borneo (Stinton, 1962; Kocsis et al., 2024), and Taiwan (Lin & Chien, 2022), ranging in age from the Miocene to the Pliocene. Siluriform bone fragments and fin spines have also been found in Java, with potential affinities to the families Clariidae and Bagridae (e.g., Hennig, 1911; Koumans, 1949), although some remains may be of ariid origin. An update on several of these Plio-Pleistocene bones from Java was provided by Yudha et al. (2020). It is worth mentioning that siluriform fossils are also known from Eocene freshwater deposits in Sumatra (Sanders, 1934).

This paper aims to describe the osteological fossil remains of Ariidae and Plotosidae found in Sarawak, and to determine their taxonomic affinities. Morphological descriptions and classifications of the fossils are based on modern comparative literature (e.g., Ohe, 2001, 2006; Aguilera et al., 2013; Marceniuk et al., 2024) and extant fishes collected from Sarawak and Brunei, comprising twelve ariid and one plotosid species, and over 200 specimens (see Material and Methods, also Supplementary Figs. S1, S2). Allometric relationships between the size of modern taxa and selected bones have been established and used to assess the size structure of the fossil fish assemblage. This work provides the first comprehensive account of fossil ariid and plotosid catfishes from Malaysian Borneo, and the findings offer valuable data for interpreting their palaeobiodiversity and ecological context.

MATERIAL AND METHODS

In the Rajang River Delta, vertebrate fossils are frequently washed up along the coastline. Our fossils were collected at low tide on the beach of Bruit Island (Fig. 1) during fieldwork conducted in November 2019 and February 2020. The vertebrate fossils comprise teeth and bones, displaying a range of altered colours, from black and grey to light brown. They were interspersed with the shells of both fossil and modern invertebrates on the beach. The vertebrate assemblage is notably diverse and is dominated by Osteichthyes, with Ariidae (sea catfish) being particularly abundant, and Chondrichthyes, represented by numerous shark and ray teeth (e.g., *Galeocerdo*, *Glyphis*, and myliobatids). Reptile fossils are also present, albeit less common, limited to a few turtle shell fragments, crocodile teeth, and snake vertebrae. Aquatic mammal fossils have also been recovered, including a possible sea cow (dugong) rib bone, cetacean epiphysis disks, and periotic ear bones.

Among the terrestrial mammal fossils, teeth of suids (e.g., *Sus barbatus* and *Sus scrofa*) and cervids (e.g., *Rusa unicolor),* as well as rarer fossils of rodents, tapirs (*Tapirus*), bantengs (*Bos*), and cercopithecids (e.g., macaques) were identified, suggesting that most of these fossils belong to extant taxa. Although some are locally extinct in Borneo (e.g., *Tapirus*), these finds support a relatively young geological age for the assemblage, approximately late Pleistocene to Holocene.

Fossil bones. Among the fish remains, ariids dominate the teleost fauna (ray-finned fish) and are the focus of this study. The collected catfish fossils were relocated from Sarawak to a laboratory in Universiti Brunei Darussalam (UBD) for detailed anatomical and taxonomic study. Most of the material is well preserved; however, some specimens are broken, fragmentary, or worn, likely having been affected by

Fig. 1. Maps of Southeast Asia and fossil locality. A, map of Borneo Island, showing Sarawak, East Malaysia, and the catfish fossil locality (in red box). B, Bruit Island [= Pulau Bruit] in the Rajang River Delta, off Sibu city (aerial image from Google Maps).

transport and reworking in the fluvial and coastal depositional environments. A subset of fossils was cleaned using an ultrasonic bath to remove adhering sediments and then was air-dried at room temperature.

More than 300 ariid and plotosid fossil bones were examined, of which 237 could be classified at the generic and species levels (Tables 1, 2). The study was divided into two parts: (1) cranial and (2) postcranial skeletal elements, the latter mainly containing dorsal and pectoral spines. Illustrations of

the best-preserved specimens were prepared using a digital microscope (VHX-7000, KEYENCE) housed at Géopolis, University of Lausanne, Switzerland. The fossil specimens are catalogued and deposited in the palaeontological collection of the Department of Geology, University of Malaya (UM), Kuala Lumpur, Malaysia, with the inventory numbers prefixed UMF-PB-, which refer to specimens of the same type of bones (Table 1). The supra-ordinal classification of Betancur-R et al. (2017) is followed in this study.

Modern bones. Over 220 modern Ariidae specimens, representing eight genera and twelve species, were collected from local fish markets in Brunei and Sarawak (Malaysia). The standard length (SL), total length (TL), and head length (HL) were recorded for each specimen, and each fish was photographed from multiple angles. The otoliths of these specimens have been studied by Johari et al. (2025). From 45 selected specimens, skeletal elements, primarily cranial bones, were prepared for comparative analysis with the fossil material (see Supplementary Figs. S3–8). The bones were extracted and cleaned using various methods, including burial for several days and boiling. Once the flesh was removed, the bones were further cleaned in a hydrogen peroxide solution. The skulls and other skeletal parts were photographed for documentation. The collected ariids and plotosids were subsequently classified based on morphological characteristics, particularly features of the head shield (e.g., the shape of the supraoccipital process), the shape and arrangement of palatine tooth patches, the number of barbels, and otolith morphology (e.g., Kailola, 1999, 2004; Ohe, 2006; Kumar et al., 2015; Marceniuk et al., 2024).

Allometric data, including linear regressions between total length (TL, or standard length - SL), skull dimensions, and the proportions of selected bones and otoliths, were utilised to estimate the body size of the fossil fishes (Table 3, Supplementary Figs. S9–S10, Tables S1–2). Arratia (2003) is followed for most of the skeletal terminology, and Ballen & De Pinna (2022) for pectoral and dorsal spines.

The following abbreviations are used in the text and figures: TL, total length in cm; HL, head length in cm; acf, anterior cranial fontanel; bo, basioccipital; eo, exoccipital; ep, epioccipital; es, extrascapular (i.e., posttemporal; see Kubicek, 2022); fr, frontal; let, lateral ethmoid; mes, mesethmoid; os, orbitosphenoid; pa, parasphenoid; pcf, posterior cranial fontanel; pls, pleurosphenoid; pr, prootic; ps, posttemporo-supracleithrum (i.e., supracleithrum; see Kubicek, 2022); pt, pterotic; sp, sphenotic; so, supraoccipital (i.e., parieto-supraoccipital); sop, supraoccipital process; tf, temporal fossa; vm, vomer; web, Weberian apparatus; OL, otolith length; OW, otolith width.

TAXONOMY

Class Actinopteri Cope, 1871

Infraclass Teleostei Müller, 1845

Order Siluriformes Cuvier, 1817

Family Ariidae Bleeker, 1858

Arius Valenciennes, 1840b

Arius cf. *maculatus*
(Fig. 2)

Material examined. One partially preserved neurocranium with the left otolith, UMF-PB-060, from Bruit Island, Sarawak (Fig. 2).

Descriptions. The anterior and posterior parts of the skull are largely lost. The mesethmoid and lateral ethmoids are not preserved, but the posterior part and part of the fenestra anterior to the frontal are visible. The anterior cranial fontanelle is large, elongated, and cylindrical in shape. It is followed by a smaller posterior cranial fontanelle and a medial groove that extends posteriorly towards the anterior part of the supraoccipital (i.e., parieto-supraoccipital). The fontanelles and the grooves extend along more than half of the neurocranium. The supraoccipital process is broken off. In dorsal view, paired cranial elements, including the frontal, sphenotic, pterotic, extrascapular, and posttemporo-supracleithra are visible. The latter three surround a well-recognisable temporal fossa. The left otic capsule is partially preserved, and the lapillus otolith has been extracted (OL: 11.6 mm, OW: 8.4 mm). The otolith is moderately worn, and features on the ventral surface are not clearly observable (Fig. 2A2). Other observable and partially preserved bones in ventral view are the basioccipital, parasphenoid, orbitosphenoid, left prootic, and exoccipital.

Remarks. Although the skull is fragmentary, the observable features most closely resemble those of *Arius maculatus* (Thunberg, 1792), based on examination of modern comparative material (Fig. 2C) and published illustrations of skulls (Marceniuk et al., 2024, fig. 24A; Lin et al., 2025, fig. 4). We additionally examined two other species of modern *Arius* from northern Bornean waters, namely *A. venosus* Valenciennes, 1840b and *A. oetik* Bleeker, 1846. The skulls of these species are narrower, with a wider anterior fontanelle, a more elongated posterior fontanelle, and a substantially larger prefrontal fenestra (Supplementary Figs. S3, S4). The ornamentation and supraoccipital processes also differ among the three species.

The otolith's shape fits the "maculatus-shape type" of Ohe (2006), which corresponds to the elongated group of Kocsis et al. (2024) and Johari et al. (2025). The otoliths of other ariid species, *Arius arius* (Hamilton, 1822), *A. oetik, A. venosus, Cryptarius truncatus* (Valenciennes, 1840b), *Pseudosciades sona* (Hamilton, 1922), and *Batrachocephalus mino* (Hamilton, 1922), have also been reported as similar (see Ohe, 2006; Johari et al., 2025).

Given the incomplete condition of the skull and the limited availability of comparable material from other *Arius* species, the fossil skull is described in open nomenclature. FishBase

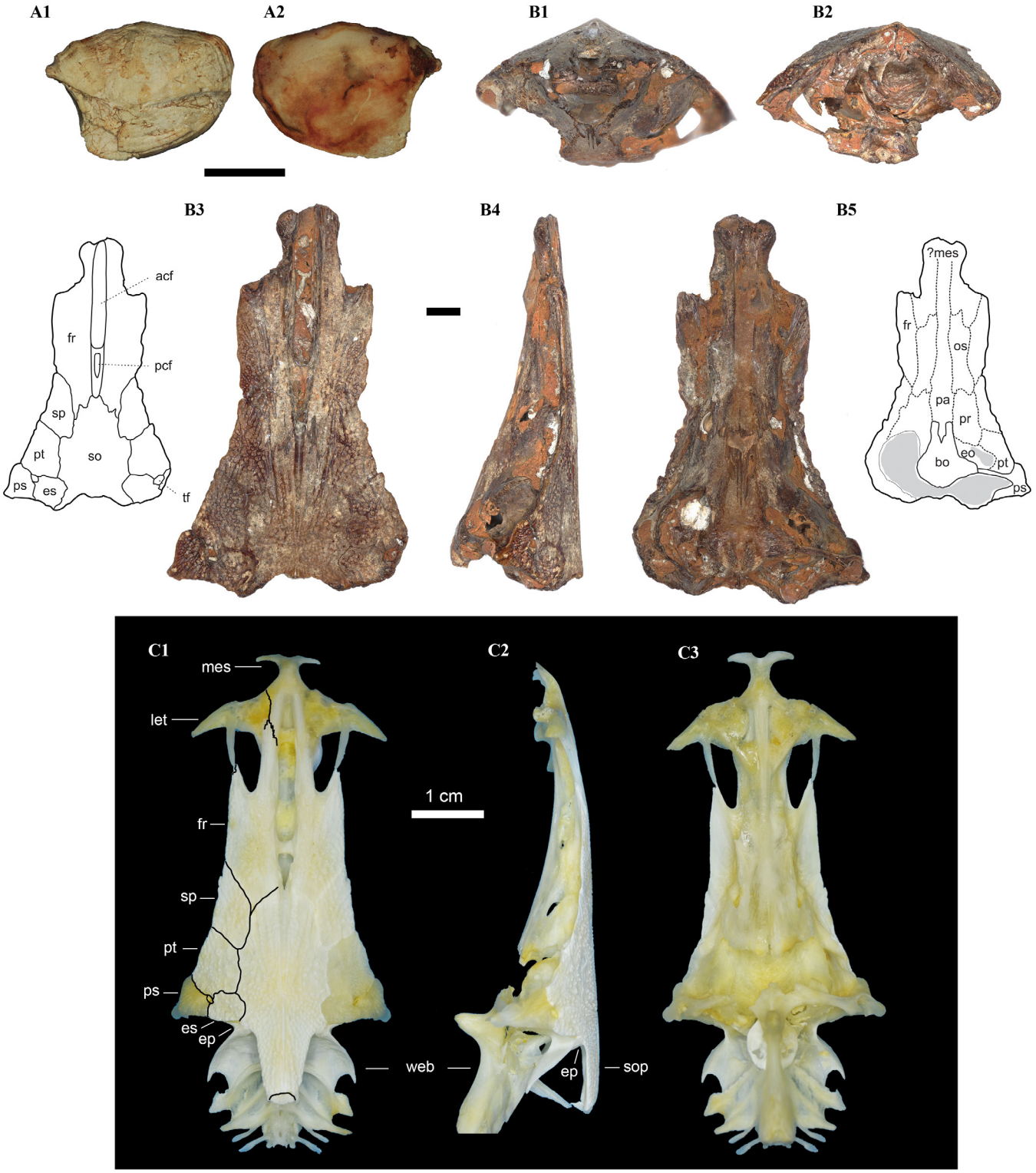

Fig. 2. Neurocrania of fossil *Arius* cf. *maculatus* and modern *Arius maculatus* from Borneo in comparison. A, B, fossil *Arius* cf. *maculatus* from Bruit Island, Sarawak (UMF-PB-060); A, left lapillus otolith in dorsal (A1) and ventral (A2) views; B, neurocranium in anterior (B1), posterior (B2), dorsal (B3), lateral (B4) and ventral (B5) views. For B3 and B5, sketches are provided. C, modern neurocranium of *Arius maculatus* from Brunei (BRUJM-20200626-7). Scale bars represent 5 mm, unless otherwise indicated. Abbreviations: see Material and Methods.

lists 26 species of *Arius* worldwide (Froese & Pauly, 2025), while the new classification of Marceniuk et al. (2024) recognises 20. In the Southeast Asian seas (Eastern Indian Ocean and Western Central Pacific), 10–14 species are expected to be present (Froese & Pauly, 2025). These species are common in shallow coastal waters, particularly in brackish and occasionally in freshwater habitats.

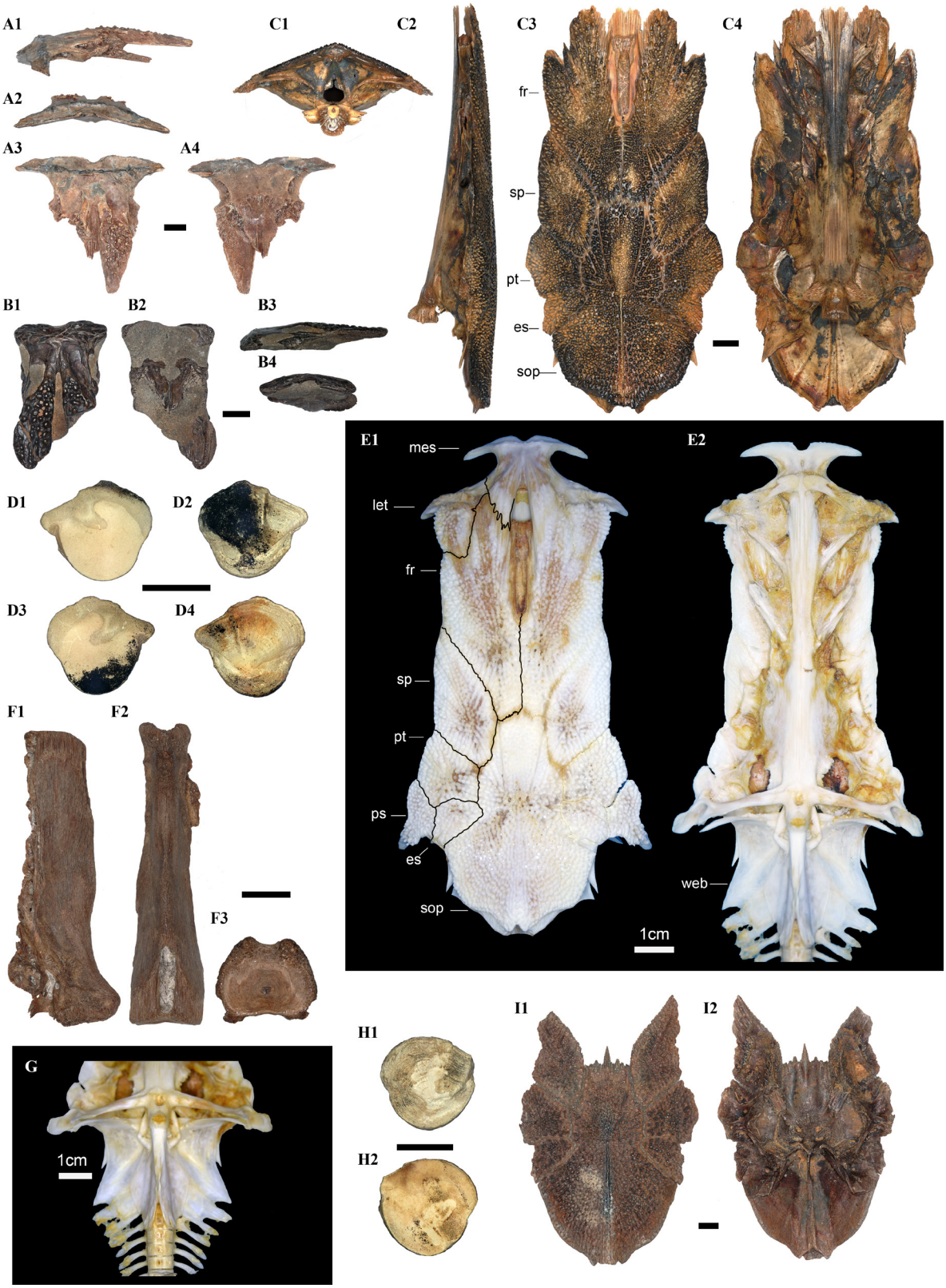

Fig. 3. Fossil and modern cranial specimens of *Hexaematichthys sagor* from Borneo in comparison. A, fossil mesethmoid from Bruit Island in lateral (A1), anterior (A2), dorsal (A3), and ventral (A4) views (UMF-PB-012). B, fossil mesethmoid in dorsal (B1), ventral (B2), lateral (B3), and anterior (B4) views (UMF-PB-013). C, entire fossil neurocranium, in posterior (C1), lateral (C2), dorsal (C3), and ventral (C4) views (UMF-PB-014). D, a pair of lapillus otoliths extracted from the fossil neurocranium shown in Fig. 3C; the right otolith (D1–D2) and the left otolith (D3–D4) in ventral and dorsal views, respectively. E, modern neurocranium of *H. sagor* in dorsal (E1) and ventral (E2) views (BRUPB-20200617-1). F, fossilised complex vertebra in lateral (F1), ventral (F2), and posterior (F3) views (UMF-PB-024). Note that this is part of the Weberian apparatus. G, close-up of the Weberian apparatus of a modern *H. sagor* in ventral view (BRUPB-20200617-1). H, a partially preserved fossil lapillus otolith acquired from a half-broken supraoccipital, with a partially preserved otic capsule and articulated sphenoid, in dorsal (H1) and ventral (H2) views (UMF-PB-016). I, posterior part of the fossil neurocranium exhibiting the articulation of the supraoccipital process, sphenoid, pterotic, and extrascapular, in dorsal (I1) and ventral (I2) views (UMF-PB-015). Scale bars represent 5 mm, unless otherwise indicated. Abbreviations: see Material and Methods.

Hexanematichthys Bleeker, 1858

Hexanematichthys sagor (Hamilton, 1822)
(Figs. 3–5)

Pimelodus sagor Hamilton, 1822: 169–170, 376.
Bagrus sagor (Hamilton, 1822) –Valenciennes, 1840a: 446.
Bagrus sondaicus Valenciennes, 1840a: 444.
Arius (*Hexanematichthys*) *sagor* (Hamilton, 1822) – Kailola, 1999: 1862.
Arius sagor (Hamilton, 1822) – Bleeker, 1846: 29; Ohe, 2006: 18, fig. 9B.
Hexanematichthys sagor (Hamilton, 1822) – Bleeker, 1858: 65; Ferraris, 2007: 45; Marceniuk et al., 2024: 453, fig. 24D.
'*Sciades*' *sagor* (Hamilton, 1922) – Betancur-R, 2009: 9, fig. 4B.

Material examined. Cranial materials (136 specimens): one nearly complete neurocranium with a pair of otoliths (lapilli), UMF-PB-014 (Fig. 3C); one partially preserved right posterior part of the cranium with sop, ex, pt, sh, right lapillus, UMF-PB-016 (Fig. 3H); one posterior part of the neurocranium with the articulation of sh, pt, ex, so, sop, UMF-PB-015 (Fig. 3I); one fr+sp, UMF-PB-031; 43 – so–sop, some are fragmented, UMF-PB-001–006; five posttemporal supracleithra (two left and three right), UMF-PB-011; nine sphenotics (four left, four right, and one unknown), UMF-PB-009); five pterotics, UMF-PB-010; 16 frontals (ten left, five right, and one unknown), UMF-PB-008; two mesethmoids, UMF-PB-012–013 (Fig. 3A–B); 34 cranial fragments, UMF-PB-017; 14 nuchal bones, UMF-PB-025–027 (Fig. 4G–H); one hyomandibular bone (right), UMF-PB-023 (Fig. 4M); three opercles, UMF-PB-028–030 (Fig. 4I–K). Postcranial bones (55 specimens): one complex vertebra, UMF-PB-024 (Fig. 3F); 24 cleithra (11 left and 13 right), UMF-PB-018–022 (Fig. 4A–D); eight dorsal spines, UMF-PB-035–036 (Fig. 5A); 22 pectoral spines (11 left and 11 right), UMF-PB-032–034 (Fig. 5C). All from Bruit Island, Sarawak.

Description. The neurocranium is flat and broad both anteriorly and posteriorly, exhibiting a rectangular shape in dorsal view. Distinctively granulated ornamentation extends from the frontal to supraoccipital process, with the granules arranged in longitudinal rows of raised ridges. A single, large, elongated cranial fontanel (i.e., medial groove) covers approximately one-third of the skull. The supraoccipital (i.e., parieto-supraoccipital) is narrow anteriorly, resembling an isosceles trapezium, and broadens posteriorly into a fan-shaped supraoccipital process. The anterior edge of this bone projects slightly between the frontal bones, ending in a pointed tip that connects with the frontals. It possesses the largest surface area among the bones covering the dorsal aspect of the neurocranium. The supraoccipital process is dorsally convex, featuring a thick central ridge. Its posterior edge is broad, circular, and fully convex, while the anterolateral region is straight where it joins the extrascapular. In posterior view, the bone bends slightly ventrally. Like other parts of the dorsal neurocranium, its ornamentation is strongly granulated with longitudinal ridges. Laterally, the bone articulates with the sphenotic, pterotic, and extrascapular bones, with no fenestra between them.

The recovered posttemporo-supracleithra are broken and worn. This bone connects the pectoral girdle to the neurocranium. The dorso-medial limb is short and broad, featuring an articulating surface that connects to the extrascapular and prootic. The pterotic is a small bone that appears roughly square in dorsal view. It articulates medially with the supraoccipital, posteriorly with the extrascapular, and anteriorly with the sphenotic. The sphenotic is stout and broad, rhomboid in shape, with sharply pointed anterior and posterior edges. It articulates anteriorly with the posterior part of the frontal. The frontal bone is flat and rectangular, broad anteriorly and tapering posteriorly to a narrow, thin end. The cranial fontanelle opens in the centre of the frontal bones and spans approximately two-thirds of their length. The anterolateral part of the mesethmoid is broad and features a median cleft. Broken fragments of the frontal with characteristic ornamentation are attached posteriorly to this bone (Fig. 3A, B).

Three otoliths were recovered from two individuals: a pair of lapilli (Fig. 3D, OL: 7.9 & 8.1 mm, OW: 7.4 & 7.3 mm, respectively left and right) and a worn right lapillus (Fig. 3H, OL: >8.1 mm, OW: 7.9 mm). They are nearly circular in shape. The pair are well-preserved, and display additional diagnostic features (Fig. 3D), including a prominent antero-mesial projection, a tubular, curved sulculus lapilli, a wide, mesial shallow depression, and a deep, bent incisura linea basalis (see also Johari et al., 2025). The third otolith is heavily worn, with its antero-mesial projection broken off (Fig. 3H).

Several postcranial skeletal elements were found. The fossilised complex vertebra (part of the Weberian complex) is an elongated bone situated between the basioccipital and the rest of the vertebral column (Fig. 3F). The bone widens and thickens posteriorly, featuring a crest-like ventral part at its centre. The cleithrum is a robust element (Fig. 4A–D) that constitutes a large portion of the pectoral girdle and forms the posterior part of the branchial chamber. It is elongated antero-posteriorly, with a broader posterior section that exhibits three prominent processes: the superior dorsal, inferior dorsal, and humeral processes. Its external surface is angular and strongly granulated, characterised by longitudinal ridges. The nuchal plate is a bony dermal expansion that flanks the dorsal fin, exhibiting a butterfly shape in dorsal view (Fig. 4G, H), with a V-shaped articulation surface that connects anteriorly to the supraoccipital process. The plate is wide and convex dorsally, adorned with granulated ornamentation. The hyomandibular bone is roughly rectangular and flat, with a well-developed dorsal process (Fig. 4M). The opercle is triangular, displaying elongated or web-like ornamentation on its external surface (Fig. 4I, K).

Out of the eight dorsal spines, two are fully preserved (Fig. 5A). They are axially symmetrical, unlike the pectoral spines. The base of the dorsal spine, along with its associated articular foramen, is triangular. The anterior and lateral sides of the spine bear large tubercules and spinules, which are arranged along ridges along the shaft. The posterior side is rather smooth with a deep groove. The shaft curves posteriorly,

Fig. 4. Postcranial elements of fossil and modern *Hexanematichthys sagor* from Borneo in comparison. A–D, three fossil cleithra from Bruit Island: A, left cleithrum in lateral (A1), mesial (A2), anterior (A3), and ventral (A4) views (UMF-PB-018); B, right cleithrum (UMF-PB-019); C, right cleithrum (UMF-PB-020); D, right cleithrum (UMF-PB-021), in lateral (1) and mesial (2) views, respectively. E, modern left cleithrum in lateral (E1–E2) and mesial (E3) views (BRUSB-20200628). F, complete modern nuchal bone in dorsal (F1), ventral (F2), and lateral (F3) views (BRUPB-20200617-1). G, H, fossil nuchal bones from Bruit Island: G, posterior fragment in dorsal (G1), ventral (G2), anterior (G3), posterior (G4), and lateral (G5) views (UMF-PB-025); H, anterior part of a nuchal bone in dorsal (H1), ventral (H2), anterior (H3), posterior (H4), and lateral (H5) views (UMF-PB-026). I–K, fossil opercles: I, J, left opercle (UMF-PB-029–030) in mesial (I1) and distal (I2) views, K, right opercle (UMF-PB-028) in mesial (K1), distal (K2), anterior (K3) views. L, modern right opercle bone in mesial (L1) and distal (L2) views (BRUPB-20200617-2). M, fossil right hyomandibular from Bruit Island in mesial (M1) and lateral (M2) views (UMF-PB-023). N, modern left hyomandibular bone in distal (N1) and mesial (N2) views (BRUPB-2018). Scale bars represent 5 mm, unless otherwise indicated.

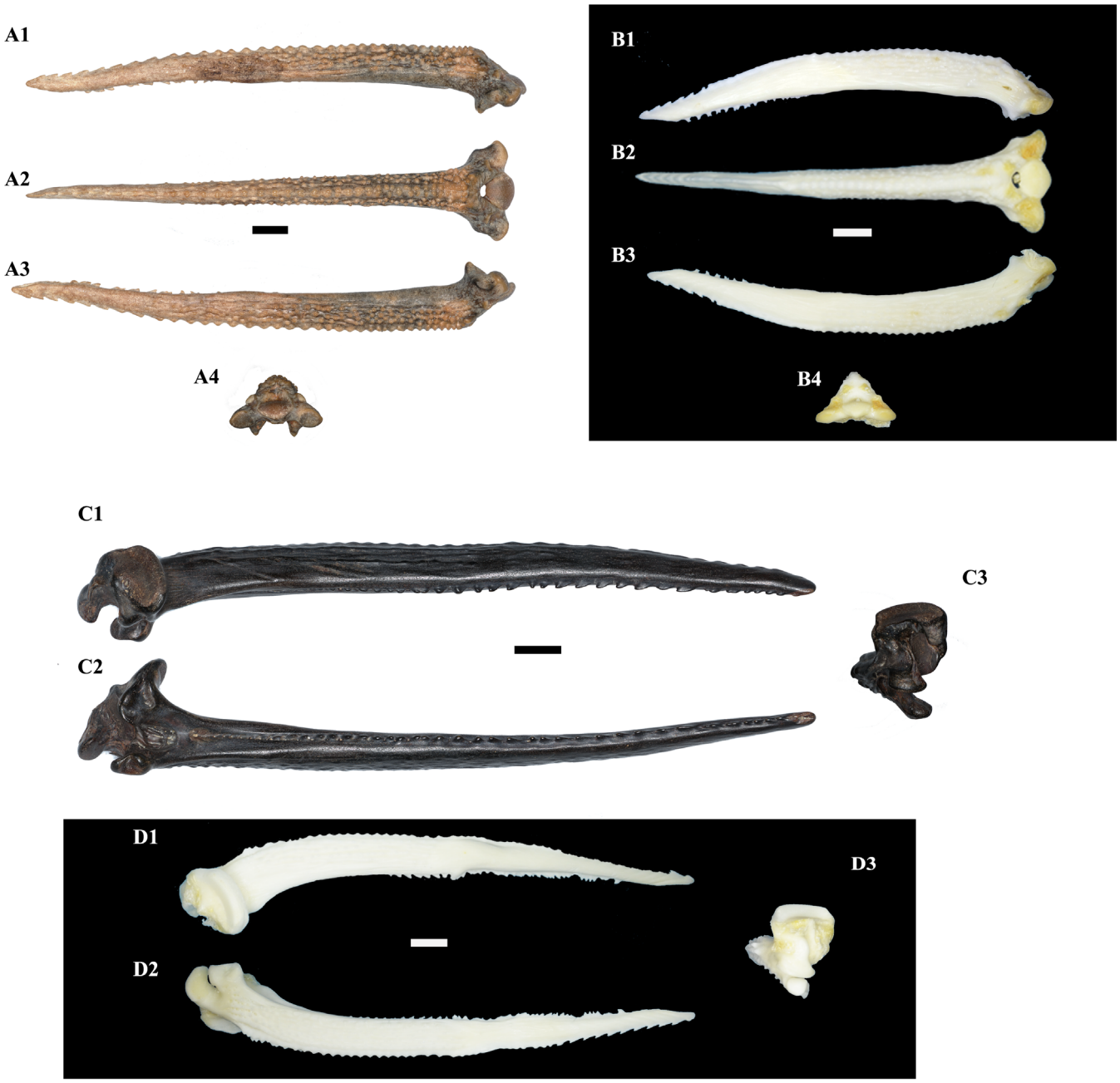

Fig. 5. Fossil and modern dorsal and pectoral spines of *Hexanematichthys sagor* from Borneo in comparison. A, fossil dorsal spine from Bruit Island (UMF-PB-035) and B, modern dorsal spine from Brunei (BRUPB-20200617-1), in left lateral (A1), anterior (A2) and right lateral (A3), and basal (4) views. C, right pectoral spine of fossil specimen from Bruit Island (UMF-PB-033) in dorsal (C1), posterior (C2), and mesial (C3) views. D, right pectoral spine of modern *H. sagor* from Brunei (BRUPB-2018) in dorsal (D1), ventral (D2), and mesial (D3) views. Scale bars represent 5 mm.

with the tip bending backwards, creating a sinusoidal shape in lateral view. Here, the spinules are flattened laterally, and the posteriormost ones form small blades. The pectoral spines exhibit similar characteristics (Fig. 5C). The spine base is asymmetrical, with a wide dorsally extended articular plateau. The posterior ornamentation shows larger blades and spinules compared to the anterior one. The dorsal and ventral surfaces are smoother and bear low ridges along the shaft. Notably, the features of the pectoral spine in *H. sagor* are also similar to those reported for some other catfish from the region (e.g., Koumans, 1949; Yudha et al., 2020).

Remarks. Several modern specimens of *H. sagor* from Brunei were examined, including eight skulls and some postcranial elements (see selected examples in Figs. 3–5, Supplementary Figs. S3–8). The recovered fossil bones are clearly identical to those of modern *H. sagor* (see also Ohe, 2006, fig. 9B; Betancur-R, 2009, fig. 4B; Marceniuk et al., 2024, fig. 24D). The shape of the otoliths ("clam-shaped type" in Ohe, 2006, or rounded-group, Ariidae indet. 1, in Kocsis et al., 2024), and their wide, symmetrically curved distal margins further confirm their affinity with modern *H. sagor* (Johari et al., 2025). While the genus *Netuma*, known from the region, has similar otoliths, their distal margin is less rounded (see Johari et al., 2025).

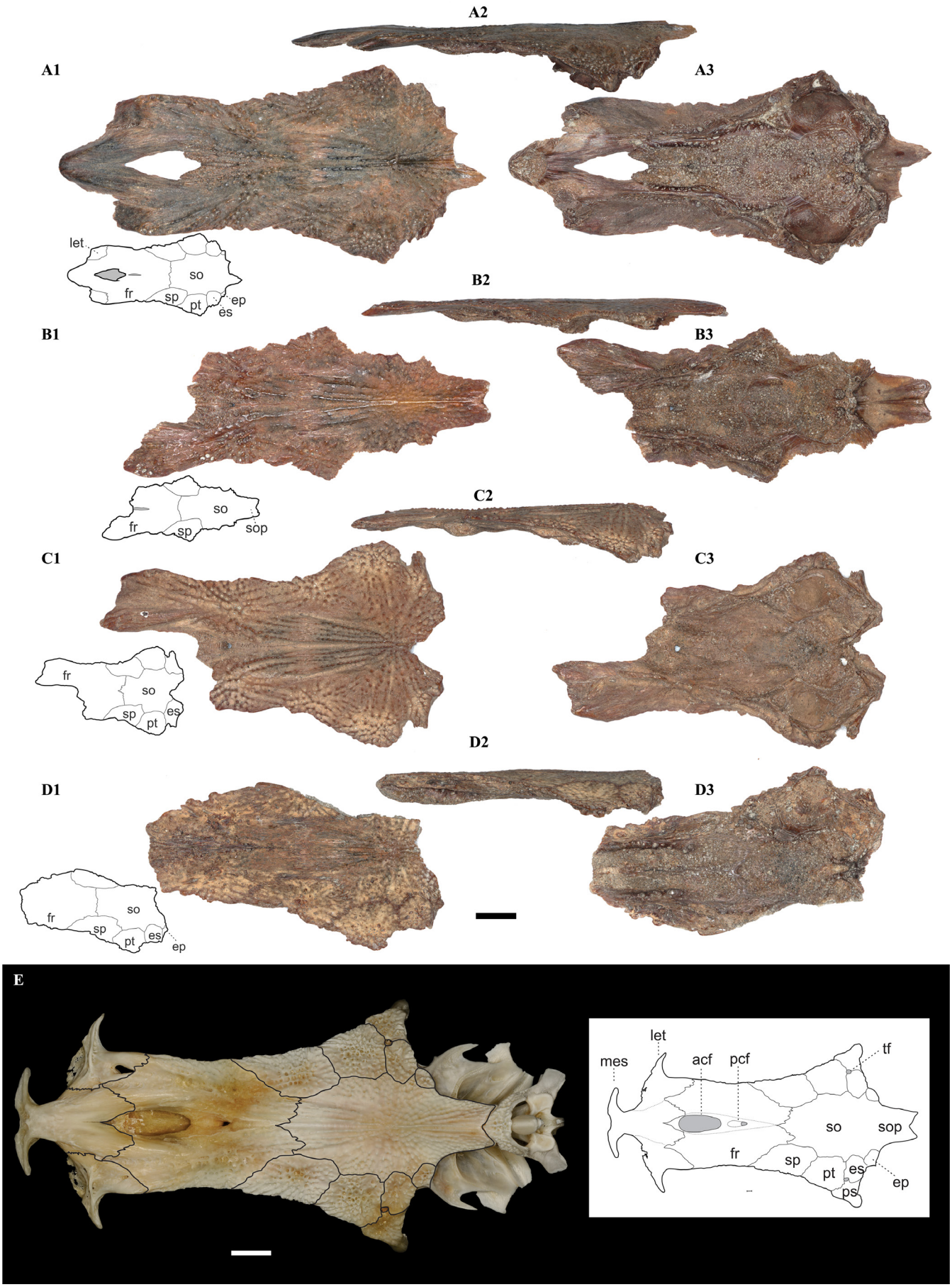

Fig. 6. Fossil and modern neurocranial remains of *Kyataphisa nenga* from Borneo in comparison. A–D, fossil specimens from Bruit Island, Sarawak, in various preservation states; A, UMF-PB-050; B, UMF-PB-051; C, UMF-PB-052; D, UMF-PB-053, from left to right in dorsal (1), ventral (2), and lateral (3) views, respectively. E, neurocranium of modern *K. nenga* from Brunei (BRUJM-20200626-14) in dorsal view. Scale bars represent 5 mm.

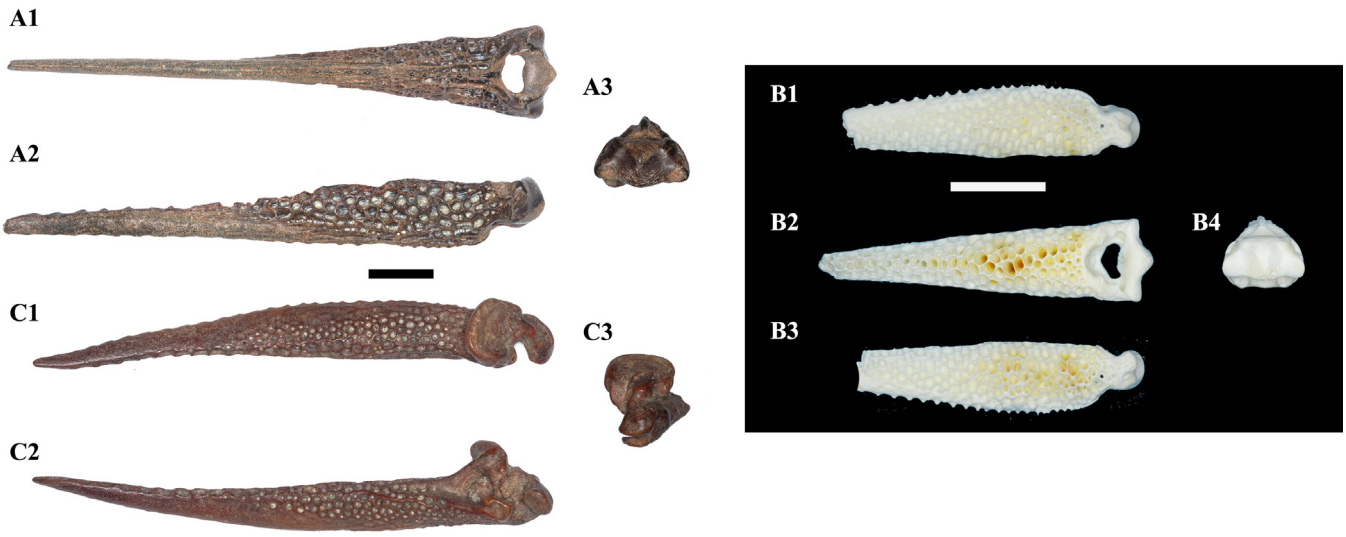

Fig. 7. Fossil and modern dorsal and pectoral spines of *Kyataphisa nenga* from Borneo in comparison. A, fossil dorsal spine from Bruit Island, Sarawak (UMF-PB-055) in anterior (A1), lateral (A2), and basal (A3) views. B, modern dorsal spine of *K. nenga* from Mukah, Sarawak (MALMU-20200228-3) in left lateral (B1), anterior (B2), right lateral (B3), and basal (B4) views. C, left pectoral spine of fossil *K. nenga* from Bruit Island (UMF-PB-058) in dorsal (C1), ventro-lateral (C2), and mesial (C3) views. Scale bars represent 5 mm.

H. sagor is a common species in the Indo-Australian Archipelago, inhabiting coastal areas and estuaries. It is currently considered the sole representative of *Hexanematichthys* (Marceniuk et al., 2024). It should be noted that the type species of *Hexanematichthys*, *Bagrus sondaicus* Valenciennes, 1840a, is here treated as a junior synonym of *H. sagor*, following Marceniuk et al. (2024). Previously, *Pararius mastersi* (Ogilby, 1898), from northern Australia and New Guinea Island, was included in *Hexanematichthys* (e.g., Ferraris, 2007), but is now retained in *Pararius* (Marceniuk et al., 2024, p. 472). *Hexanematichthys henni* Fisher & Eigenmann in Eigenmann, 1922, reported from South America, has been classified as a junior synonym of *Chinchaysuyoa labiata* (Boulenger, 1898) by Marceniuk et al. (2019) or is considered an uncertain identification (Froese & Pauly, 2025).

Kyataphisa Marceniuk et al., 2024

Kyataphisa nenga (Hamilton, 1822)
(Figs. 6, 7)

Pimelodus nenga Hamilton, 1822: 171–172, 376.
Arius nenga (Hamilton, 1822) – Bleeker, 1858: 68; Kailola, 1999: 1859; Ohe, 2006: 20, fig. 11B; Betancur-R, 2009: 9, fig. 4A.
Nemapteryx nenga (Hamilton, 1822) – Kailola, 2004: 1399; Ferraris, 2007: 47.
Kyataphisa nenga – Marceniuk et al., 2024: 453, fig. 24E.

Material examined. Cranial materials: Four fragmentary neurocrania, UMF-PB-050–053 (Fig. 6A–D); postcranial bones: four dorsal spines (one complete), UMF-PB-055–056; eight pectoral spines (six left, two right), UMF-PB-057–059 (Fig. 7A, C). All from Bruit Island, Sarawak.

Description. The fragmentary neurocrania are small, measuring less than 5 cm in length. The best-preserved specimen (UMF-PB-050) exhibits an overall trapezoidal shape with a wider posterior end (Fig. 6A). The anterior cranial fontanelle is oval-shaped, followed by a much smaller, more elliptical posterior cranial fontanelle. Several cranial bones can be identified, although not all are visible in each of the four specimens. The supraoccipital is short (Fig. 6B), bordered by the frontal, sphenotic, pterotic, and extrascapular bones. In two specimens, part of the epioccipital is visible at the posterior end. The ornamentation of the neurocrania predominantly consists of randomly arranged tubercles, although some exhibit a slight linear pattern. The supraoccipital bone features longitudinal ridges that extend to the frontals, forming a V-shape.

The foramen of the dorsal spine is flattened and triangular. The bone itself is thin and narrow. A key characteristic is the presence of deep alveoli that cover most of the surface of the shaft (Fig. 7). The pectoral spine is also thin and narrow, with comparable ornamentation.

Remarks. The fossil specimens exhibit most diagnostic features of extant *Kyataphisa nenga* (Hamilton, 1822) (see Ohe, 2006, fig. 11B; Betancur-R, 2009, fig. 4A; Marceniuk et al., 2024, fig. 24E). We examined six modern specimens of the species, of which four had their skulls prepared for anatomical comparison—three from Sarawak (Mukah and Bruit Island) and one from Brunei (Fig. 6E, Supplementary Figs. S3, S4). While the overall skull morphology is very similar, certain variations are observed among these modern specimens. The dot-like ornamentation is more pronounced and coarser in some specimens (Supplementary Fig. S3F), whereas others exhibit additional web-like ornamentation in specific regions, particularly on the sphenotic and pterotic (Fig. 6E). Another variation involves the dorsal visibility of the epioccipital bone: in some specimens, it is clearly visible with a distinct suture (Fig. 6E), while in others, it is not apparent (Supplementary Fig. S3F). The epioccipital is also evident in recently published illustrations of *K. nenga* (as shown in Betancur-R, 2009; Marceniuk et al., 2024), further supporting the identification of these fossil

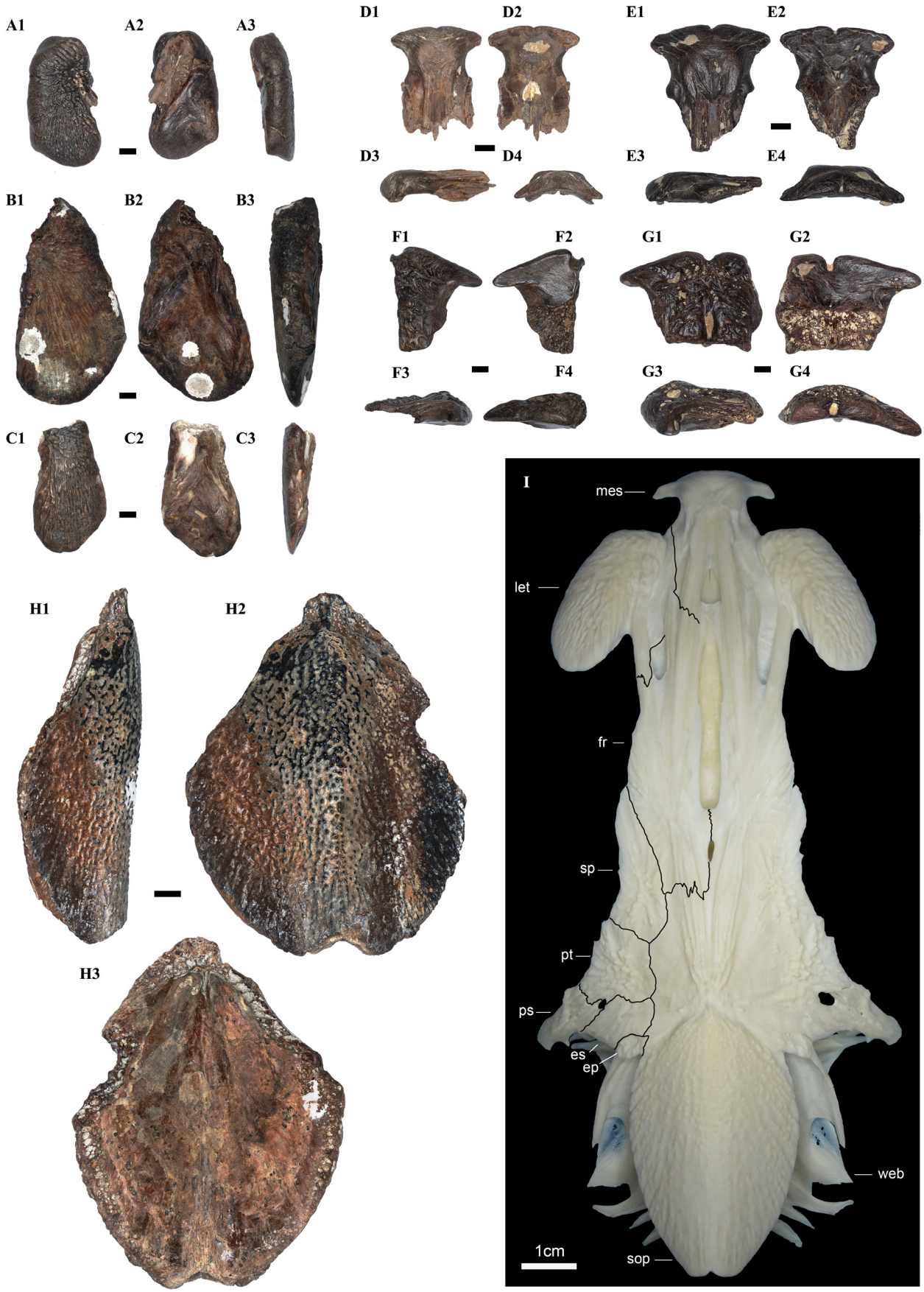

Fig. 8. Fossil and modern cranial bones of *Plicofollis nella* and *P.* aff. *nella* from Borneo in comparison. A–E, fossil *Plicofollis nella* from Bruit Island, Sarawak; A–C, left and right lateral ethmoids, in dorsal (1), ventral (2) and lateral (3) views (UMF-PB-037–039); D, E, fossil mesethmoid bones, in dorsal (1), ventral (2), lateral (3) and anterior (4) views (UMF-PB-043–044); F, G, fossil mesethmoid bones of *Plicofollis* aff. *nella* from Bruit Island, in dorsal (1), ventral (2), lateral (3), and anterior (4) views (UMF-PB-045–046). H, fossil supraoccipital process of *P. nella* from Bruit Island, in lateral (1), dorsal (2) and ventral (3) views (UMF-PB-041); I, neurocranium of modern *P. nella* from Brunei in dorsal view (BRUJM-20200713-1). Scale bars represent 5 mm, unless otherwise indicated.

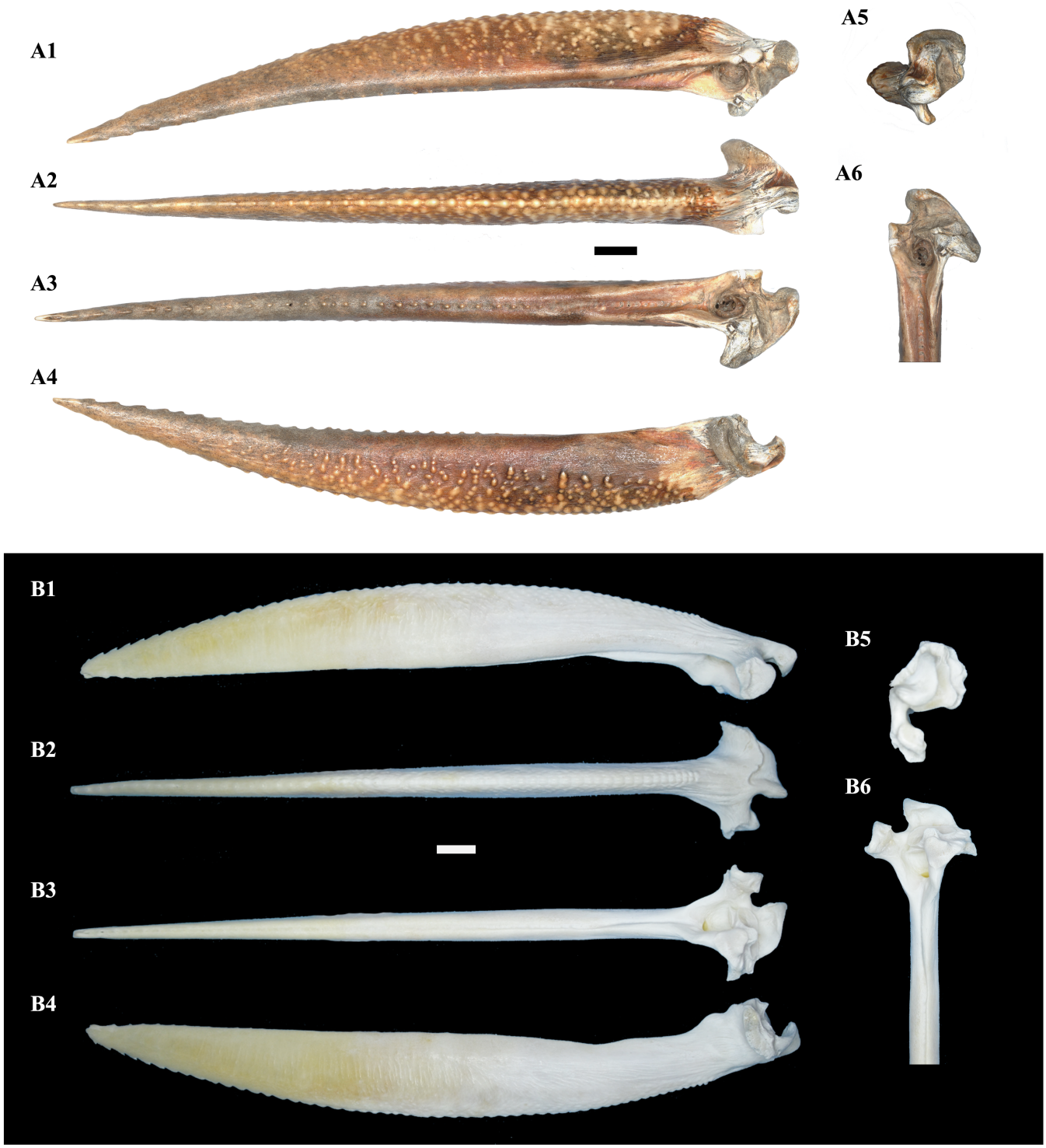

Fig. 9. Right pectoral spines of fossil and modern *Plicofollis nella* from Borneo in comparison. A, fossil spine from Bruit Island, Sarawak (UMF-PB-047). B, modern specimen from Brunei (BRUGM-20200622) in ventral (1), anterior (2), posterior (3), dorsal (4), and mesial (5) views, close up on the articulation (6). Scale bars represent 5 mm.

specimens. Whether the observed differences among the modern specimens reflect natural variation within the species (e.g., population differences, ontogenetic stages, and/or sexual dimorphism) or represent taxon-specific traits remains to be confirmed through molecular studies.

K. nenga [originally in *Pimelodus*] was previously placed in the genus *Nemapteryx* (e.g., Kailola, 2004; Ferraris, 2007) and has also been discussed under *Arius* (e.g., Betancur-R, 2009). The genus *Kyataphisa* was recently established by Marceniuk et al. (2024) to include only *K. nenga*. On the other hand, FishBase includes *Kyataphisa caelata* (Valenciennes, 1840b) and recognises the issue that this species may represent a junior synonym of *K. nenga* (see Kailola, 2004; Marceniuk et al., 2024; Froese & Pauly, 2025). *K. nenga* is widespread in coastal marine and brackish waters across South Asia and Southeast Asia (Marceniuk et al., 2024).

Kyataphisa cf. *nenga*

Remarks. Four neurocranium fragments from Bruit Island, Sarawak, UMF-PB-054, were available. These fossils are worn and represent the broken anterior ends of the supraoccipital bone. These bones resemble those of *K. nenga*; however, due to their insufficient state of preservation, they are described with open nomenclature.

Plicofollis Kailola, 2004

Plicofollis nella (Valenciennes, 1840b)
(Figs. 8, 9)

Pimelodus? *nella* Valenciennes, 1840b: 162–163.
"*Arius*" *nella* (Valenciennes, 1840b) – Kailola, 1999: 1858.
Arius leiotetocephalus Bleeker – Ohe, 2001: 40, fig. 2; Ferraris, 2007, 52.
Arius nenga (Hamilton, 1822) – Ohe, 2006: 17, fig. 9A.
Plicofollis nella (Valenciennes, 1840b) – Kailola, 2004: 141; Ferraris, 2007: 52; Lin et al., 2025: 90, fig. 8.

Material examined. Cranial materials: Three supraoccipital processes, UMF-PB-041–042 (one complete – Fig. 8H, and two fragments); two mesethmoids (i.e., ethmoid & dermethmoid), UMF-PB-043–044 (Fig. 8D–E); 12 lateral ethmoids (three left, six right, and three uncertain fragments), UMF-PB-037–040 (Fig. 8A–C); Post-cranial bones: four poorly preserved dorsal spines, UMF-PB-049; two right pectoral spines, UMF-PB-047–048 (Fig. 9A). All from Bruit Island, Sarawak.

Description. The supraoccipital bone is large (7 cm long, 5.3 cm wide) and exhibits a drop-like shape in dorsal view. It displays a pronounced ventral bend, characterised by a small, sharp curve at the posterior end where it articulates with the nuchal plate. The ornamentation primarily consists of radially arranged striae. The mesethmoid is robust, featuring a bulky medial portion and a distinct medial cleft with a rounded anterior margin. The lateral ethmoids are large and elongated antero-posteriorly, presenting a broad, kidney-like shape, and are adorned with long, radially arranged striae that originate from the anterior portion.

The dorsal spine is wide and slender, characterised by a deep groove on its posterior side. The articular foramen is minute. The spine is ornamented with fine tubercles. The pectoral spine is also wide and slender, exhibiting a wedge-like shape (Fig. 9A). Its anterior surface is more heavily ornamented, while the posterior groove is marked by small tubercules.

Remarks. Most of these osteological features are characteristic of *Plicofollis nella* (Fig. 8I; Ohe, 2001, fig. 2; Ohe, 2006, fig. 8A; Lin et al., 2025, fig. 8). The enlarged, elongated lateral ethmoids are particularly distinctive when compared to other catfish (Supplementary Figs. S3, S4). The large and wide supraoccipital process is also a key anatomical trait. Notably, the shape of this bone changes throughout ontogeny, becoming wider (i.e., decreasing in a length/width ratio) (Lin et al., 2025).

FishBase lists eight modern *Plicofollis* species, five of which inhabit the broader Indo-Australian Archipelago (Froese & Pauly, 2025). We examined several modern specimens of the two common species *P. nella* (n = 19) and *P. argyropleuron* (Valenciennes, 1840b) (n = 5) from Brunei waters (Fig. 8I, Supplementary Figs. S2–S4). The largest modern specimen of *P. nella* in our collection measured over 60 cm (TL). In fact, *P. nella* is among the largest ariid catfish species in our South China Sea collection, second only to *Netuma thalassina* (Rüppell, 1837) and *N. bilineata* (Valenciennes, 1840a) (Supplementary Fig. S2).

Plicofollis aff. *nella*
(Fig. 8F–G)

Cranial materials. Two mesethmoids, UMF-PB-045–046 from Bruit Island, Sarawak (Fig. 8F–G).

Description. These fragmentary mesethmoids are larger and more robust than those confidently assigned to *P. nella* (Fig. 8D–E). While the lateral surface displays similar horizontal lineations, the dorsal surface is more coarsely ornamented, exhibiting a rather web-like pattern. The medial cleft is also more pronounced compared with the aforementioned specimens of *P. nella*.

Remarks. The observed differences may be the result of taphonomic processes (e.g., abrasion) and/or ontogenetic variation. Thus, these bones may belong to a large *P. nella*. However, based on available comparative material, our six modern skulls of *P. nella* from Brunei and published data (e.g., Ohe, 2001; Lin et al., 2025), such dorsal ornamentation has not been observed on the mesethmoids of even the largest specimens. Therefore, these bones are either heavily eroded elements of *P. nella* or may represent a different, as yet unidentified, species of *Plicofollis*.

Family Plotosidae Bleeker, 1858

Plotosus Lacépède, 1803

Plotosus cf. *canius*
(Fig. 10)

Material examined. One mesethmoid, UMF-PB-062; One parasphenoid bone, UMF-PB-063; Vomer articulated with parasphenoid, UMF-PB-064, all from Bruit Island, Sarawak (Fig. 10).

Description. The tip of a small mesethmoid was recovered, characterised by a U-shape formed by its anterolateral projections (Fig. 10A). A small central extension is present on the ventral surface. Although the posterior portion is incomplete, a medial groove is observable, representing the anterior tip of the frontal fontanelle. The fragmentary parasphenoid is an elongated bone exhibiting a crest-like feature along its ventral surface (Fig. 10B). The vomer is distinctly triangular and articulated with the anterior end of the parasphenoid (Fig. 10C).

Table 1. List of the siluriform (catfish) fossil specimens from Bruit Island, Borneo, examined in this study.

Cat. No.	Family	Taxon	Material	Number	Notes
UMF-PB-001	Ariidae	*Hexanematichthys sagor*	supra occipitale process (sop)	1	Fig 11A
UMF-PB-002	Ariidae	*Hexanematichthys sagor*	supra occipitale process (sop)	1	Fig 11B
UMF-PB-003	Ariidae	*Hexanematichthys sagor*	supra occipitale process (sop)	1	Fig 11C
UMF-PB-004	Ariidae	*Hexanematichthys sagor*	supra occipitale process (sop)	1	Fig 11D
UMF-PB-005	Ariidae	*Hexanematichthys sagor*	supra occipitale process (sop)	1	Fig 11E
UMF-PB-006	Ariidae	*Hexanematichthys sagor*	supra occipitale processes (sop)	15	few are fragmentary
UMF-PB-007	Ariidae	*Hexanematichthys sagor*	supra occipitale process (sop)	23	fragments
UMF-PB-008	Ariidae	*Hexanematichthys sagor*	frontal fragments (fr)	16	one with sediment
UMF-PB-009	Ariidae	*Hexanematichthys sagor*	Sphenotic (sp)	9	
UMF-PB-010	Ariidae	*Hexanematichthys sagor*	Pterotic (pt)	5	
UMF-PB-011	Ariidae	*Hexanematichthys sagor*	Posttemporal Supracleithrum (ps)	5	
UMF-PB-012	Ariidae	*Hexanematichthys sagor*	Mesethmoid (mes)	1	Fig. 3A
UMF-PB-013	Ariidae	*Hexanematichthys sagor*	Mesethmoid (mes)	1	Fig. 3B
UMF-PB-014	Ariidae	*Hexanematichthys sagor*	neurocranium without the anterior part, and 2 otoliths	1	Fig. 3C, otoliths — Fig. 3D
UMF-PB-015	Ariidae	*Hexanematichthys sagor*	posterior part of the neurocranium	1	Fig. 3I
UMF-PB-016	Ariidae	*Hexanematichthys sagor*	right posterior of the cranium (sop + otic capsule) + otolith	1	otolith — Fig. 3H (only otolith)
UMF-PB-017	Ariidae	*Hexanematichthys sagor*	cranial fragments	34	
UMF-PB-018	Ariidae	*Hexanematichthys sagor*	Cleithrum	1	Fig. 4A
UMF-PB-019	Ariidae	*Hexanematichthys sagor*	Cleithrum	1	Fig. 4B
UMF-PB-020	Ariidae	*Hexanematichthys sagor*	Cleithrum	1	Fig. 4C
UMF-PB-021	Ariidae	*Hexanematichthys sagor*	Cleithrum	1	Fig. 4D
UMF-PB-022	Ariidae	*Hexanematichthys sagor*	Cleithrum	20	some fragmentary
UMF-PB-023	Ariidae	*Hexanematichthys sagor*	Hyomandibula - right	1	Fig. 4M
UMF-PB-024	Ariidae	*Hexanematichthys sagor*	Complex vertebra	1	Fig. 3F
UMF-PB-025	Ariidae	*Hexanematichthys sagor*	Nuchal bones	1	Fig. 4G
UMF-PB-026	Ariidae	*Hexanematichthys sagor*	Nuchal bones	1	Fig. 4H
UMF-PB-027	Ariidae	*Hexanematichthys sagor*	Nuchal bones	12	most are fragmented
UMF-PB-028	Ariidae	*Hexanematichthys sagor*	Opercle	1	Fig. 4K
UMF-PB-029	Ariidae	*Hexanematichthys sagor*	Opercle	1	Fig. 4I
UMF-PB-030	Ariidae	*Hexanematichthys sagor*	Opercle	1	Fig. 4J
UMF-PB-031	Ariidae	*Hexanematichthys sagor*	cranial part: frontal + sphenotic	1	
UMF-PB-032	Ariidae	*Hexanematichthys sagor*	left pectoral spines	11	
UMF-PB-033	Ariidae	*Hexanematichthys sagor*	right pectoral spines	1	Fig. 5C
UMF-PB-034	Ariidae	*Hexanematichthys sagor*	right pectoral spines	10	
UMF-PB-035	Ariidae	*Hexanematichthys sagor*	dorsal spine	1	Fig. 5A
UMF-PB-036	Ariidae	*Hexanematichthys sagor*	dorsal spines	7	
UMF-PB-037	Ariidae	*Plicofollis nella*	lateral ethmoid (let)	1	Fig. 8A

Cat. No.	Family	Taxon	Material	Number	Notes
UMF-PB-038	Ariidae	*Plicofollis nella*	lateral ethmoid (let)	1	Fig. 8B
UMF-PB-039	Ariidae	*Plicofollis nella*	lateral ethmoid (let)	1	Fig. 8C
UMF-PB-040	Ariidae	*Plicofollis nella*	lateral ethmoid (let)	9	
UMF-PB-041	Ariidae	*Plicofollis nella*	supra occipitale process (sop)	1	Fig. 8H
UMF-PB-042	Ariidae	*Plicofollis nella*	supra occipitale processes (sop)	2	
UMF-PB-043	Ariidae	*Plicofollis nella*	Mesethmoid (mes)	1	Fig. 8D
UMF-PB-044	Ariidae	*Plicofollis nella*	Mesethmoid (mes)	1	Fig. 8E
UMF-PB-045	Ariidae	*Plicofollis* aff. *nella*	Mesethmoid (mes)	1	Fig. 8F
UMF-PB-046	Ariidae	*Plicofollis* aff. *nella*	Mesethmoid (mes)	1	Fig. 8G
UMF-PB-047	Ariidae	*Plicofollis nella*	right pectoral spine	1	Fig. 9A
UMF-PB-048	Ariidae	*Plicofollis nella*	right pectoral spine	1	
UMF-PB-049	Ariidae	*Plicofollis nella*	dorsal spines	4	worn and fragmentary remains
UMF-PB-050	Ariidae	*Kyataphisa nenga*	neurocranial fragment	1	Fig. 6A
UMF-PB-051	Ariidae	*Kyataphisa nenga*	neurocranial fragment	1	Fig. 6B
UMF-PB-052	Ariidae	*Kyataphisa nenga*	neurocranial fragment	1	Fig. 6C
UMF-PB-053	Ariidae	*Kyataphisa nenga*	neurocranial fragment	1	Fig. 6D
UMF-PB-054	Ariidae	*Kyataphisa* cf. *nenga*	neurocranial fragments	4	
UMF-PB-055	Ariidae	*Kyataphisa nenga*	dorsal spine	1	Fig. 7A
UMF-PB-056	Ariidae	*Kyataphisa nenga*	dorsal spines	3	
UMF-PB-057	Ariidae	*Kyataphisa nenga*	right pectoral spines	2	
UMF-PB-058	Ariidae	*Kyataphisa nenga*	left pectoral spine	1	Fig. 7C
UMF-PB-059	Ariidae	*Kyataphisa nenga*	left pectoral spines	5	
UMF-PB-060	Ariidae	*Arius* cf. *maculatus*	neurocranial fragment with left otolith preserved	1	Fig. 2A–B
UMF-PB-061	Ariidae	Ariidae indet.	vertebras	9	
UMF-PB-062	Plotosidae	*Plotosus* cf. *canius*	Mesethmoid (mes)	1	Fig. 10A
UMF-PB-063	Plotosidae	*Plotosus* cf. *canius*	Parasphenoid bone	1	Fig. 10B
UMF-PB-064	Plotosidae	*Plotosus* cf. *canius*	Vomer articulated with the parasphenoid	1	Fig. 10C
UMF-PB-065	Ariidae	Ariidae indet.	pectoral and dorsal spine fragments	28	some might be *Kyataphisa*
UMF-PB-066	Ariidae	Ariidae indet.	pectoral and dorsal spine fragments	38	one with joint to the cleithrum
UMF-PB-067	Ariidae	Ariidae indet.	opercles	2	
UMF-PB-068	Ariidae	Ariidae indet.	bone fragments: 8 cranial, 1 cleithrum	9	some might be *H. sagor*
			total:	**326**	

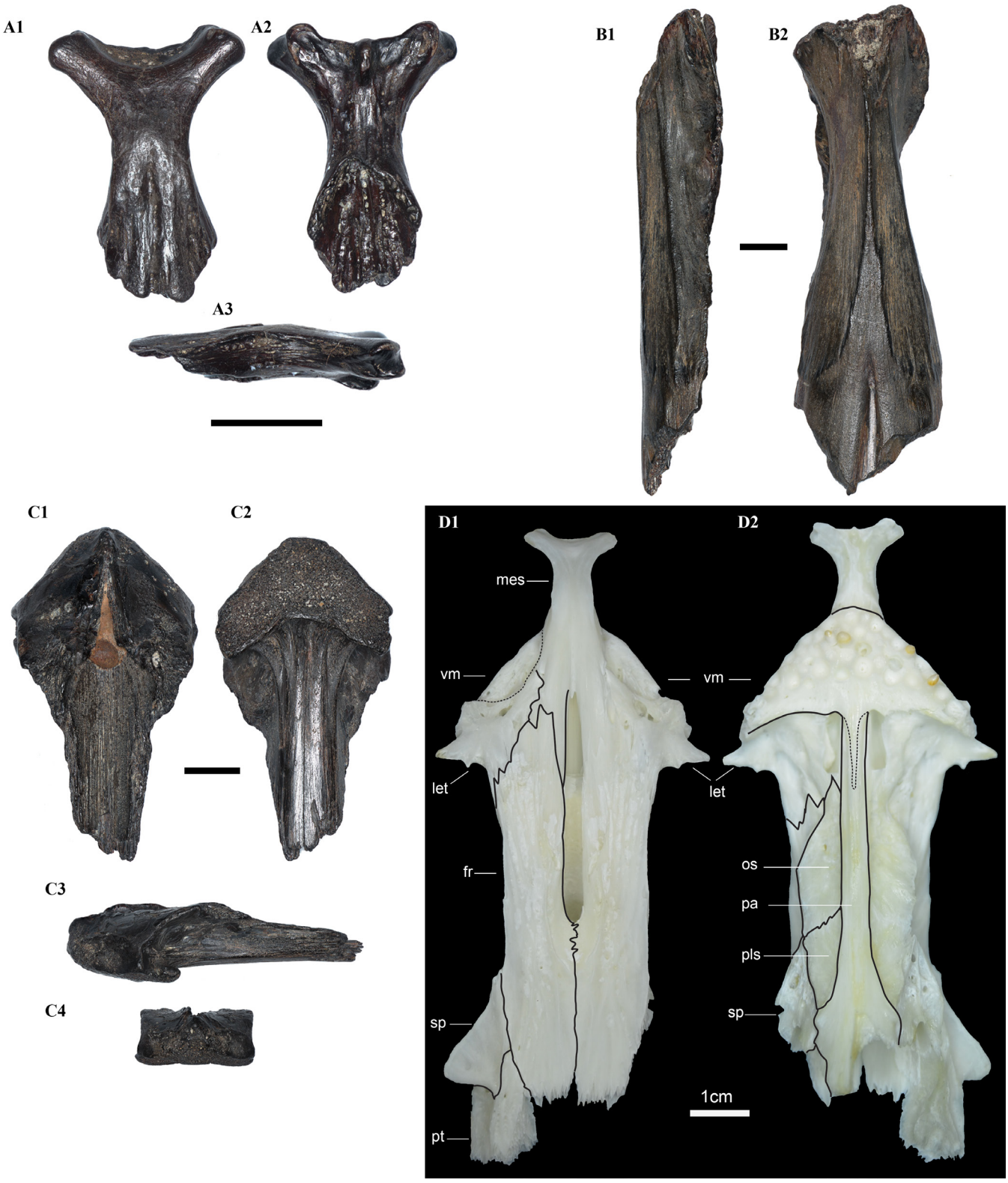

Fig. 10. Fossil and modern bones of *Plotosus* from Borneo in comparison. A–C, cranial bones elements of fossil *Plotosus* cf. *canius* from Bruit Island, Sarawak: A, mesethmoid bone in dorsal (A1), ventral (A2), and lateral (A3) views (UMF-PB-062); B, parasphenoid bone in lateral (B1) and ventral (B2) views (UMF-PB-063); C, vomer articulated with the parasphenoid in dorsal (C1), ventral (C2), lateral (C3), and anterior (C4) views (UMF-PB-064). D, neurocranium of modern *P. canius* from Brunei, in dorsal (D1) and ventral (D2) views (BRUGM20200703-3). Scale bars represent 5 mm, unless otherwise indicated.

Remarks. The articulated, triangular vomer, and the distinctive morphology of the mesethmoid are diagnostic features of the genus *Plotosus*. These elements closely resemble those of *Plotosus canius* Hamilton, 1822 (Fig. 10D). However, owing to a paucity of comparative material from other plotosid species, the species identification of these fossils is left in open nomenclature. *P. canius* is an amphidromous catfish found in Southeast Asia. While commonly found in freshwater environments, adults and larger individuals frequently migrate into marine habitats (Ferraris, 1999; Riede, 2004; Hortle & Phommanivong, 2021).

Table 2. Sum of the recovered fossil bones of the Ariidae and Plotosidae from Bruit Island, Borneo, according to different taxa and their sample numbers, percentages per collection, and types of skeletal remains.

Family	Taxon	No.	%	cranial	postcranial	
					spine	other
Ariidae	*Hexanematichthys sagor*	191	58.6	136	30	25
	Plicofollis nella & cf. *P. nella*	25	7.7	19	6	–
	Kyataphisa nenga & cf. *K. nenga*	20	6.1	8	12	–
	Arius cf. *maculatus*	1	0.3	1	–	–
	Ariidae indet.	86	26.4	10	66	10
Plotosidae	*Plotosus* cf. *canius*	3	0.9	3		
		326		**177**	**114**	**35**

DISCUSSION

The fossil fish assemblage recovered from the Rajang Delta, Borneo, comprises 326 bones belonging to the order Siluriformes, primarily from the families Ariidae (323 specimens) and Plotosidae (3) (Table 1). Many bones (86 specimens), including cranial elements, spines, and vertebrae, exhibit affinities with the Ariidae, however, their incomplete preservation precludes further classification. Conversely, the remaining ariid specimens, consisting of 237 bones (73%), were identified to the generic and/or species levels; namely, *Hexanematichthys sagor* (191), *Plicofollis nella* and *P.* aff. *nella* (25), *Kyataphisa nenga* and *K.* cf. *nenga* (20), and *Arius* cf. *maculatus* (1). These identifications are primarily based on cranial elements, and, with the exception of *H. sagor*, postcranial bones are represented solely by the dorsal and lateral spines (Table 2).

Size structure of the ariid assemblage. *Hexanematichthys sagor* is the most abundant species in this fossil fauna, comprising 58.6% of the specimens. It is represented by individuals of varying sizes, as evidenced by elements such as the cleithra (Fig. 4A–D) and the supraoccipital bones (Fig. 11). Based on the skulls of five modern specimens and the otoliths of ten modern specimens (TL: 21–46 cm) (Supplementary Table S1), several allometric relationships were evaluated (Table 3). Using the dimensions of the skull, supraoccipital (SO) bone, and otolith, a total length of 31.6 ± 1.6 cm was estimated for the best-preserved fossil specimen (UMF-PB-014, Fig. 3C–D, Table 3). Among the five measured parameters, the otolith length yielded the lowest estimate (30.4 cm), while the otolith width produced the highest (34.0 cm). Two other partially preserved specimens were estimated to have TLs of 37.8 ± 0.3 cm (UMF-PB-015, Fig. 3I) and 37.3 ± 0.1 cm (UMF-PB-016, Fig. 3H), based on three and two parameters, respectively (Table 3). These allometric estimates are consistent with the size range observed in the modern dataset.

Although the number of modern skull specimens is relatively small (n = 5, Table 3, Supplementary Table S2), they provide a useful baseline for assessing the size structure of *H. sagor* within the fossil assemblage. The SO bone is the most common cranial element in our fossil record, and twenty specimens were utilised to calculate estimated TLs. Both SO length and width were measured, and the resulting TL estimates were plotted as a histogram (Fig. 11). The SO length generally yielded somewhat lower size estimates than those derived from the SO width. Nevertheless, the average TL is approximately 36 cm, with most individuals (n = 14–16) falling within a range of 30 to 40 cm. The smallest fossil specimen is estimated to be approximately 24 cm in total length, while the largest individual is estimated to reach nearly 60 cm, which is exceptional for *H. sagor* (Fig. 11). The reported average length of modern *H. sagor* is about 30 cm, but the maximum size recorded is only 45 cm long (see Kailola, 2004; Froese & Pauly, 2025). The fossil fauna from Bruit Island nevertheless reflects a size structure dominated by regular-sized individuals. The absence of juvenile catfish remains in the Bruit fossil deposit may suggest that small individuals were not part of the primary depositional assemblage (i.e., palaeo-nursery grounds could be elsewhere) or alternatively represent taphonomic artefacts.

Plicofollis nella is the second most abundant ariid species in this assemblage, accounting for 7.7% of the material. Among the cranial elements, the lateral ethmoids are the most common, with specimens of varying sizes (Fig. 8A–C). Based on our modern skull collection (n = 5, Table 3, Supplementary Table S1) and the allometric relationship involving the lateral ethmoid and the supraoccipital process, the fossil specimens represent a TL size ranging from 45.4 to 73.4 cm. According to FishBase, the maximum TL for the species is 47 cm (Froese & Pauly, 2025), although a larger standard length (SL) of 75 cm has been reported by Kailola (1999). Our largest modern specimen of *P. nella* reaches 78 cm in TL (see Johari et al., 2025), and additional records from Taiwan show individuals with a maximum SL of 68 cm (Lin et al., 2025). The fossil TL estimates from Bruit Island clearly fall within the upper size range for *P. nella*, and the absence of smaller individuals is notable.

Modern skulls of *Kyataphisa nenga* were used to estimate the original skull lengths of four partially preserved cranial

Table 3. Allometric relationships between total length (TL) and various skeletal components of modern ariid specimens, and their application in estimating the TL of selected fossil remains. The original dataset is provided in Supplementary Tables S1, S2.

	Relationship between Total Length (TL) and listed parameters						**Fossil specimens from Pulau Bruit**			
	TL vs	**slope**	**intercept**	**R^2**	**n**	**TL range (cm)**	**Estimated TL (cm)**			
							UMF-PB-014	**UMF-PB-015**	**UMF-PB-016**	
Hexanematichthys sagor	Skull length	0.2655	6.7157	0.93	5	21.0–43.0	30.6	37.6	–	
	SO length	0.9114	-6.7339	0.94	5	21.0–43.0	30.5	37.7	–	
	SO width	0.8374	8.9286	0.97	5	21.0–43.0	32.4	38.1	37.4	
	Otolith width	5.69	-7.81	0.85	10	21.0–46.0	34.0	–	37.2	
	Otolith length	4.82	-8.10	0.84	10	21.0–46.0	30.4	–	–	
						Av.	**31.6**	**37.8**	**37.3**	
						Stdev.	**1.6**	**0.3**	**0.1**	
							UMF-PB-038	**UMF-PB-37**	**UMF-PB-40**	**UMF-PB-041**
Plicofollis nella	SOP length	0.9736	4.3318	1.00	5	17.5–63.4	–	–	–	71.8
	SOP width	1.0316	11.4825	0.97	5	17.5–63.4	–	–	–	66.3
	LAT length	1.0556	10.0951	0.99	5	17.5–63.4	75.0	49.5	45.7	–
	LAT width	1.7676	13.1999	0.98	5	17.5–63.4	71.9	48.7	45.2	–
						Av.	**73.4**	**49.1**	**45.4**	**69.0**
						Stdev.	**2.2**	**0.5**	**0.3**	**3.9**
							UMF-PB-050	**UMF-PB-051**	**UMF-PB-052**	**UMF-PB-053**
Kyataphisa nenga	Skull length	0.3740	-2.2986	1.00	4	20.5–38.3	19.9	19.0	22.5	22.9
							UMF-PB-060			
Arius maculatus	Skull length	0.3528	-0.7537	0.97	4	19.4–25.9	27.5			
	Otolith width	3.7901	-4.3013	0.85	12	17.1–26.1	27.5			
	Otolith length	2.8815	-4.7117	0.85	12	17.1–26.1	28.7			
						Av.	**27.9**			
						Stdev.	**0.7**			

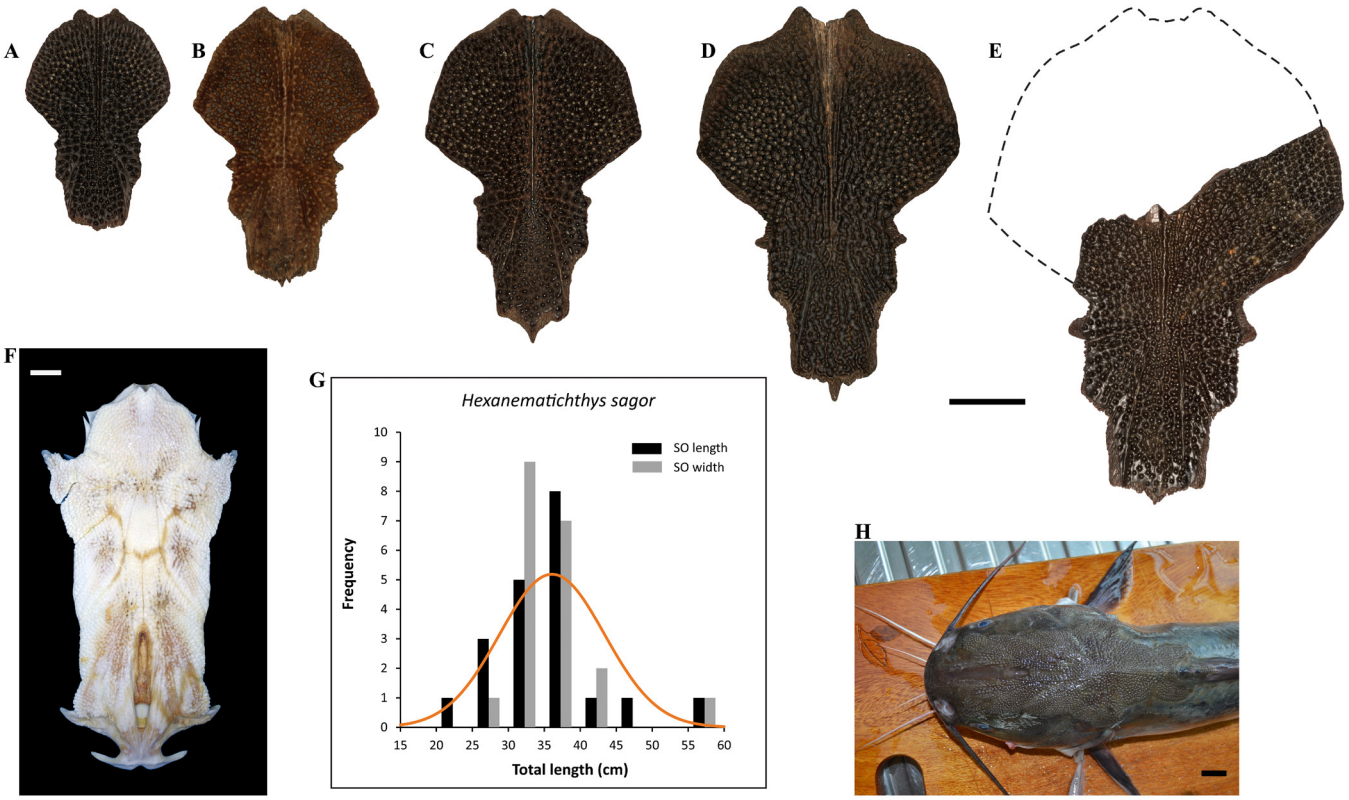

Fig. 11. Fossil and modern bones of *Hexanematichthys sagor* from Borneo. A–E, supraoccipital bones of fossil *H. sagor* from Bruit Island, Sarawak, in different ontogenetic stages, from A representing the smallest specimen and E the largest, while B to D represent intermediate sizes (A–E: UMF-PB-001–005). F, skull of modern *H. sagor* (BRUPB-20200617-1) from Brunei. G, histogram of estimated total lengths based on the length and width of 20 fossil supraoccipital bones from Bruit Island. H, head of *H. sagor* (BRUJM-20200110-1). Scale bars represent 10 mm.

fragments (Fig. 6, Supplementary Fig. S10, Tables S1, S2). Using the allometric relationship between skull length and TL based on four modern specimens (TL: 20.5–38.3 cm), the fossil samples were estimated to have TLs ranging from 19.0 to 22.9 cm (Table 3). The largest modern specimen reported is approximately 30 cm in TL (Kailola, 1999; Froese & Pauly, 2025).

For the single specimen of fossil *Arius* cf. *maculatus*, both a skull fragment and an associated otolith were used to estimate the total length, resulting in a TL of 27.9 ± 0.7 cm (Table 3). Typical specimens of modern *A. maculatus* reach 25–30 cm in TL (Froese & Pauly, 2025; Lin et al., 2025), with a reported maximum SL of 40 cm (Kailola, 1999; Froese & Pauly, 2025). It is of note that an exceptional TL of 80 cm has been reported for a specimen of this species from Oman (Randall, 1995).

Habitat range. All the four identified sea catfish taxa, along with one eeltail catfish assigned to *Plotosus* cf. *canius*, are commonly found in Southeast Asia. The first species, *Hexanematichthys sagor*, which varies in size, is the most abundant in our records. Modern *H. sagor* inhabits coastal areas, primarily around estuaries, and it ascends into the freshwater of the upper tidal zone of rivers. Its diet consists mainly of invertebrates and small fishes (Fischer & Bianchi, 1984; Kailola, 1999; Froese & Pauly, 2025). The second species, *Plicofollis nella*, is also common in coastal seas and may occur in estuaries, with a diet largely comprising sea urchins (Kailola, 1999). The third species, *Kyataphisa nenga*, inhabits inshore turbid waters, near estuaries, and is also observed in the tidal reaches of rivers (Kailola, 1999). The fourth species, *Arius maculatus*, also occurs in inshore waters, estuaries, and tidal river zones. It occasionally forms schools and feeds on invertebrates and small fishes (Fischer & Bianchi, 1984; Kailola, 1999; Froese & Pauly, 2025). Additionally, the modern eeltail catfish *Plotosus canius* typically inhabits freshwater, lagoons, and estuaries. Upon reaching a large adult size, it migrates into marine environments (Kailola, 1999; Hortle & Phommanivong, 2021).

The aforementioned habitat ranges of these species overlap significantly in coastal estuarine environments, such as the present-day Rajang River Delta, where the fossils were reworked to Bruit Island, a major tidal sand bar (Fig. 1). Therefore, the origin of the fossil catfish fauna presented here is strongly linked to the earlier deposit(s) of the Rajang deltaic system.

Origin of the fossils. The overall fossil vertebrate assemblage found on the beach of Bruit Island is dominated by fish bones and teeth, along with fossils of reptiles and mammals. These remains reflect a wide range of palaeo-habitats, encompassing fully marine (e.g., sharks, dolphins), brackish (e.g., some ariid sea catfish), freshwater (e.g., eeltail catfish), and terrestrial (e.g., boars, deer) environments. The mixed nature of the fauna, coupled with the lack of in-situ fossiliferous

layers, complicates a precise age estimation of the fossils. Nevertheless, the close resemblance of the recovered taxa to modern forms and the hitherto absence of apparent extinct taxa suggest that their age is probably no older than the late Pleistocene.

The presence of vertebrate remains from distinctly different habitats, all exposed within the beach environment, points to a variety of transport processes. Terrestrial and freshwater vertebrate remains may have been carried by rivers such as the Rajang and its tributaries. Skeletal remains of shallow marine vertebrates are likely to have been deposited in-situ within shallow coastal settings, while the carcasses of more open-water species may have been transported shoreward by currents before settling in the same shallow milieu. Wave and tidal actions likely contributed further to the mixing of remains in these transitional environments.

Glacial sea-level fluctuations must also be taken into account. During glacial maxima, Borneo was connected to mainland Southeast Asia (i.e., Sundaland, most recently around 400,000 years ago; Voris, 2000; Husson et al., 2020) and expanded river systems, combined with a retreating shoreline, may have facilitated the deposition of terrestrial fossils. Conversely, during interglacial higher sea-level stands, these lowland areas were inundated, allowing for the reworking and further mixing of vertebrate remains, potentially leading to enrichment through winnowing processes. Therefore, the mixing of older material from previous glacial-interglacial cycles may have also occurred.

Nevertheless, the dominance of estuarine catfish taxa and the absence of apparent differences in wear and preservation within the assemblage are more consistent with limited time-averaging and transport, suggesting deposition during an interglacial when estuaries and shoreline positions resembled those of the present day. Consequently, the catfish fossils may represent a relatively recent assemblage. To the best of our knowledge, this is the first diverse vertebrate fossil assemblage ever discovered in Borneo outside of cave deposits. The presence of ariid fossils is expected and further supports the interpretation of transitional, inshore, and estuarine environmental conditions, which still prevail along the Bornean coastlines today.

In conclusion, we present here a new fossil catfish fauna as part of a mixed coastal marine-terrestrial fossil assemblage of a Pleistocene/Holocene age from Bruit Island, Sarawak, Borneo, comprising over 320 bones. The catfish assemblage is predominantly Ariidae (sea catfishes), with the four taxa identified: *Hexanematichthys sagor*, *Plicofollis nella*, *Kyataphisa nenga*, and *Arius* cf. *maculatus*. Additionally, fossils of one Plotosidae (eeltail catfish), reported here as *Plotosus* cf. *canius*, were also recovered. An allometric approach, utilising modern faunas for comparison, was applied to estimate size variation among the ariid species. Based on the composition of the fauna, we infer a coastal marine environment with estuarine influence, comparable to the transitional setting in the present-day Rajang River Delta.

ACKNOWLEDGEMENTS

The research was supported by the following grants: L.K and I.H received funding from Universiti Brunei Darussalam (UBD/RSCH/1.4/FICBF(b)/2019/023); L.K. was also supported by the Fondation Agassiz from the University of Lausanne; M.S. received support from the Fundamental Research Grant Scheme (FRGS/1/2022/WAB07/UM/02/1) provided by the Ministry of Higher Education Malaysia; and M.R. received a grant from Volkswagen Stiftung AZ. 90 978. The authors would like to thank Alison Murray and an anonymous reviewer for their constructive reviews of this manuscript.

SUPPLEMENTARY DATA

All supplementary data may be obtained at the following link: www.doi.org/10.6084/m9.figshare.32055678

LITERATURE CITED

Acero PA & Betancur-R R (2007) Monophyly, affinities, and subfamilial clades of sea catfishes (Siluriformes: Ariidae). Ichthyological Exploration of Freshwaters, 18(2): 133.

Aguilera OA, Moraes-Santos H, Costa S, Ohe F, Jaramillo C & Nogueira A (2013) Ariid sea catfishes from the coeval Pirabas (Northeastern Brazil), Cantaure, Castillo (Northwestern Venezuela), and Castilletes (North Colombia) formations (early Miocene), with description of three new species. Swiss Journal of Palaeontology, 132(1): 45–68. www.doi.org/10.1007/s13358-013-0052-4

Aguilera O, Lopes RT, Rodriguez F, dos Santos TM, Rodrigues-Almeida C, Almeida P, Machado AS & Moretti T (2020) Fossil sea catfish (Siluriformes; Ariidae) otoliths and in-skull otoliths from the Neogene of the Western Central Atlantic. Journal of South American Earth Sciences, 101: 102619. www.doi.org/10.1016/j.jsames.2020.102619

Arratia G (2003) Catfish head skeleton. An overview. In: Arratia G, Kapoor BG, Chardon M & Diogo R (eds.) Catfishes, vol. 1. Science Publishers, Enfield, NH, pp. 3–46.

Ballen GA & De Pinna MCC (2022) A standardized terminology of spines in the order Siluriformes (Actinopterygii: Ostariophysi). Zoological Journal of the Linnean Society, 194(2): 601–625. www.doi.org/10.1093/zoolinnean/zlab008

Betancur-R R, Acero A, Bermingham E & Cooke R (2007) Systematics and biogeography of New World sea catfishes (Siluriformes: Ariidae) as inferred from mitochondrial, nuclear, and morphological evidence. Molecular Phylogenetics and Evolution, 45(1): 339–357. www.doi.org/10.1016/j.ympev.2007.02.022

Betancur-R R (2009) Molecular phylogenetics and evolutionary history of ariid catfishes revisited: a comprehensive sampling. BMC Evolutionary Biology, 9(1): 1–18. www.doi.org/10.1186/1471-2148-9-175

Betancur-R R, Wiley EO, Arratia G, Acero A, Bailly N, Miya M, Lecointre G & Orti G (2017) Phylogenetic classification of bony fishes. BMC Evolutionary Biology, 17(162): 1–40. www.doi.org/10.1186/s12862-017-0958-3

Bleeker P (1846) Siluroideorum bataviensium conspectus diagnosticus. Overzicht der Siluroieden, welke te Batavia voorkommen. Verhandelingen van het Bataviaasch Genootschap van Kunsten en Wetenschappen, 21(5): 1–60.

Bleeker P (1858) De visschen van den Indischen Archipel. Beschreven en toegelicht. Siluri. Acta Societatis Regiae Scientiarum Indo-Neêrlandicae, 4: 1–370.

Boulenger GA (1898) Viaggio del Dr. Enrico Festa nell'Ecuador e regioni vicine. Poissons de l'Équateur. (Première Partie). Bollettino dei Musei di Zoologia ed Anatomia Comparata della R. Università di Torino, 13(329): 1–13.

Cope ED (1871) Contribution to the ichthyology of the Lesser Antilles. Transactions of the American Philosophical Society 14(3): 445–483.

Cowman PF (2014) Historical factors that have shaped the evolution of tropical reef fishes: a review of phylogenies, biogeography, and remaining questions. Frontiers in Genetics, 5(394): 1–15. www.doi.org/10.3389/fgene.2014.00394

Cuvier G (1817) Le règne animal distribué d'après son organisation, pour servir de base à l'histoire naturelle des animaux et d'introduction à l'anatomie comparée. Avec figures, dessinées d'après nature. Tome II. Contenant les reptiles, les poissons, les mollusques et les annélides. Deterville, Paris, 532 pp.

Diogo R (2005) Adaptations, homoplasies, constraints, and evolutionary trends: catfish morphology, phylogeny and evolution, a case study on theoretical phylogeny and macroevolution. Science Publishers Inc, Enfield, USA, pp. 491.

Eigenmann CH (1922) The fishes of western South America, Part I. The fresh-water fishes of northwestern South America, including Colombia, Panama, and the Pacific slopes of Ecuador and Peru, together with an appendix upon the fishes of the Rio Meta in Colombia. Memoirs of the Carnegie Museum, 9(1): 1–346, 38 pls.

El-Sayed SE, Kora MA, Sallam HM, Claeson KM, Seiffert ER & Antar MS (2017) A new genus and species of marine catfishes (Siluriformes; Ariidae) from the upper Eocene Birket Qarun Formation, Wadi El-Hitan, Egypt. PLoS ONE 12(3): e0172409. www.doi.org/10.1371/journal.pone.0172409

El-Sayed S, Murray AM, Kora MA, Abu El-Kheir GA, Antar MS, Seiffert ER & Sallam HM (2020) Oldest Record of African Bagridae and Evidence from Catfishes for a Marine Influence in the Late Eocene Birket Qarun Locality 2 (BQ-2), Fayum Depression, Egypt, Journal of Vertebrate Paleontology, 40(2): e1780248. www.doi.org/10.1080/02724634.2020.1780248

Ferraris C (1999) Plotosidae. Eeltail catfishes (also eel catfishes, stinging catfishes, and coral catfishes). In: Carpenter KE & Niem VH (eds.) FAO species identification guide for fishery purposes. The living marine resources of the Western Central Pacific. Volume 3. Batoid fishes, chimaeras and bony fishes part 1 (Elopidae to Linophrynidae). Rome, FAO, pp. 1880–1883.

Ferraris CJ (2007) Checklist of catfishes, recent and fossil (Osteichthyes: Siluriformes), and catalogue of siluriform primary types. Zootaxa, 1418: 1–628. www.doi.org/10.11646/zootaxa.1418.1.1

Fischer W & Bianchi G (eds.) (1984) Ariidae. FAO species identification sheets for fishery purposes. Western Indian Ocean fishing area 51. Vol. 1. Introductory material, Bony Fishes Families: Acanthuridae to Clupeidae. FAO, Rome, 47 pp.

Frizzell DL (1965) Otoliths of new fish (*Vorhisia vulpes*, n. gen., n. sp. Siluroidei?) from Upper Cretaceous of South Dakota. Copeia, 1965(2): 178–181.

Froese R & Pauly D (2025) FishBase. www.fishbase.org (Accessed 30 September 2025)

Frost GA (1925) Description of fish otoliths from the Tertiary formations of Atcheen, Northern Sumatra. Wetenschappelijke mededeelingen Dienst van den Mijnbouw in Nederlandsch-Oost Indië, 2: 1–28.

Gayet M & Meunier FJ (2003) Paleontology and palaeobiogeography of catfishes. In: Arratia G, Kapoor BG, Chardon M & Diogo R (eds.) Catfishes, volume 2. Science Publishers, Enfield, NH, pp. 491–522.

Hamilton F (1822) An account of the fishes found in the river Ganges and its branches. A. Constable and Company, Edinburgh, i-vii + 1–405 pp., pls 1–39.

Hennig E (1911) Die Fischreste. In: Selenka L & Blanckenhorn M (eds.) Die Pithecanthropus-Schichten auf Java. Geologische und paläontologische Ergebnisse der Trinil-Expedition (1907 und 1908). Verlag Von Wilhelm Engelmann, Leipzig, pp. 54–60.

Hortle KG & Phommanivong S (2021) The first record from Laos of *Plotosus canius* (Teleostei: Plotosidae). Ichthyological Exploration of Freshwaters, 30(4): 377–384. www.doi.org/10.23788/IEF-1167

Huddleston RW & Savoie M (1983) Teleostean otoliths from the Late Cretaceous (Maastrichtian Age) Severn Formation of Maryland. Proceedings of the Biological Society of Washington, 96(4): 658–663. Husson L, Boucher FC, Sarr A-C, Sepulchre P & Cahyarini SY (2020) Evidence of Sundaland's subsidence requires revisiting its biogeography. Journal of Biogeography, 47: 843–853. www.doi.org/10.1111/jbi.13762

Hutchison CS (2005) Geology of North-West Borneo: Sarawak, Brunei and Sabah. Elsevier, Amsterdam, 421 pp.

Johari A, Kocsis L, Roslim A & Ilman H (2025) Otolith morphometric analysis of North Bornean Ariidae (Siluriformes): new insights and taxonomic implications. Zootaxa, 5660 (4): 451–474. www.doi.org/10.11646/zootaxa.5660.4.1

Kailola PJ (1999) Ariidae (= Tachysuridae). Sea catfishes (fork-tailed catfishes). In: Carpenter KE & Niem VH (eds.) FAO species identification guide for fishery purposes. The living marine resources of the Western Central Pacific. Volume 3. Batoid fishes, chimaeras and bony fishes, part 1 (Elopidae to Linophrynidae). Rome, FAO, pp. 1827–1879.

Kailola PJ (2004) A phylogenetic exploration of the catfish family Ariidae. The Beagle: Records of the Museums and Art Galleries of the Northern Territory, 20: 87–166. www.doi.org/10.5962/p.286323

Kocsis L, Lin C-H, Bernard E & Johari A (2024) Late Miocene teleost fish otoliths from Brunei Darussalam (Borneo) and their implications for palaeoecology and palaeoenvironmental conditions. Historical Biology, 36(12): 2642–2676. www.doi.org/10.1080/08912963.2023.2271489

Koumans FP (1949) On some fossil fish remains from Java. Zoologische Mededeelingen, 30(5): 77–82.

Kubicek KM (2022) Developmental osteology of *Ictalurus punctatus* and *Noturus gyrinus* (Siluriformes: Ictaluridae) with a discussion of siluriform bone homologies. Vertebrate Zoology, 72: 661–727. www.doi.org/10.3897/vz.72.e85144

Kumar R, Jaiswar AK, Chakraborty SK, Sarkar UK & Lakra WS (2015) Morphological differentiation of catfishes of the family Ariidae occurring along the west coast of India. Indian Journal of Fisheries, 62(4): 109–115.

Lacépède BGE (1803) Histoire naturelle des poissons. Tome Cinquième. Chez F. G. Levrault, Paris, pp. 1–803.

Lin C-H & Chien C-W (2022) Late Miocene otoliths from northern Taiwan: Insights into the rarely known Neogene coastal fish community of the subtropical northwest Pacific. Historical Biology, 34(2): 361–382. www.doi.org/10.1080/08912963.2021.1916012

Lin C-H, Tseng Y-C, Ho H-C, Mediodia DP, Lee C-H, Yang S-H & Chang C-H (2025) Taxonomic review of the sea catfish family Ariidae in Taiwan. Marine Research of the National Academy of Marine Research, 5(1): 75–140. www.doi.org/10.29677/MR.202506_5(1).0004

Marceniuk AP & Menezes NA (2007) Systematics of the family Ariidae (Ostariophysi, Siluriformes), with a redefinition of the genera. Zootaxa, 1416: 1–126. www.doi.org/10.11646/zootaxa.1416.1.1

Marceniuk AP, Menezes NA & Britto MR (2012) Phylogenetic analysis of the family Ariidae (Ostariophysi: Siluriformes), with

a hypothesis on the monophyly and relationships of the genera. Zoological Journal of the Linnean Society, 165(3): 534–669. www.doi.org/10.1111/j.1096-3642.2012.00822.x

Marceniuk AP, Marchena J, Oliveira C & Betancur-R R (2019) *Chinchaysuyoa*, a new genus of the fish family Ariidae (Siluriformes), with a redescription of *Chinchaysuyoa labiata* from Ecuador and a new species description from Peru. Zootaxa, 4551(3): 361–378. www.doi.org/10.11646/zootaxa.4551.3.5

Marceniuk AP, Oliveira C & Ferraris CJ Jr (2024) A new classification of the family Ariidae (Osteichthyes: Ostariophysi: Siluriformes) based on combined analyses of morphological and molecular data. Zoological Journal of the Linnean Society, 200: 426–476. www.doi.org/10.1093/zoolinnean/zlad078

Müller J (1845) Über den Bau und die Grenzen der Ganoiden, und über das natürliche System der Fische. Archiv für Naturgeschichte, 11(1): 91–141.

Nelson JS, Grande TC & Wilson MVH (2016) Fishes of the World. 5th Edition. John Wiley and Sons, Hoboken, 707 pp. www.doi.org/10.1002/9781119174844.

Ogilby JD (1898) New genera and species of fishes. Proceedings of the Linnean Society of New South Wales, 23(1): 32–41.

Ohe F (2001) Osteological data of living fishes to the Pliocene marine catfish (Family Ariidae). Kaseki no Tomo, 48: 38–43.

Ohe F (2006) Skulls and otoliths of eleven sea catfishes (Family Ariidae) from Malaysia and one species related to them from the East China Sea. Natural Environmental Science Research, 19: 11–28.

Peyer B (1928) Die Welse des ägyptischen Altterti ärs nebst einer kritischen Übersicht über alle fossilen Welse. Abhandlungender Bayerischen Akademie der Wissenschaften, Mathematischnaturwissenshaftliche Abteilung, 32:1–61.

Randall JE (1995) Coastal fishes of Oman. University of Hawaii Press, Honolulu, Hawaii, 439 pp.

Rao VR (1956) The skull of an Eocene siluroid fish from Western Cutch, India, Journal of the Palaeontological Society of India, 1(1): 181–185.

Riede K (2004) Global register of migratory species - from global to regional scales. Final Report of the R&D-Projekt 808 05 081. Federal Agency for Nature Conservation, Bonn, Germany, 329 pp.

Rüppell WPES (1837) Neue Wirbelthiere zu der Fauna von Abyssinien gehörig. Fische des Rothen Meeres. Siegmund Schmerber, Frankfurt am Main, pp. 53–80.

Sahni A & Mishra VP (1975) Lower Tertiary vertebrates from Western India. Monograph of the Palaeontological Society of India. Monograph no. 3. Palaeontological Society of India, Lucknow, pp. 1–48.

Sanders M (1934) Die Fossilen Fische der Alttertiären Süsswasserablagerungen aus Mittel-Sumatra. Verhandelingen van het geologisch-mijnbouwkundig genoostschap voor Nedeland en Kolonien, Geologische Series, 1: 1–144.

Stinton FC (1962) Teleostean otoliths from the Upper Tertiary strata of Sarawak, Brunei and North Borneo. British Borneo Geological Survey, Annual Report, 1962. Government Printing Office, Kuching, pp. 75–92.

Sullivan JP, Lundberg JG & Hardman M (2006) A phylogenetic analysis of the major groups of catfishes (Teleostei: Siluriformes) using rag1 and rag2 nuclear gene sequences. Molecular Phylogenetics and Evolution, 41: 636–662. www.doi.org/10.1016/j.ympev.2006.05.044

Thunberg CP (1792) Tvånne Japanske fiskar. Kongliga Vetenskaps-Academiens Handlingar, Stockholm, 13: 29–32.

Valenciennes A (1840a) [dated 1839]. Suite du livre seizième. Labroïdes. Livre dix-septième. Des Malacoptérygiens, Des Siluroïdes. In: Cuvier G & Valenciennes A (eds.) Histoire naturelle des poissons. Tome quatorzième. V. Berger-Levrault, Strasbourg, pp. 1–464, pls. 389–420.

Valenciennes A (1840b) Suite du livre dix-septième. Siluroïdes. In: Cuvier G & Valenciennes A (eds.) Histoire naturelle des poissons. Tome quinzième. V. Levrault, Strasbourg, pp. 1–540, pls. 421–455.

Voris KH (2000) Maps of Pleistocene sea levels in Southeast Asia: shorelines, river systems and time durations. Journal of Biogeography, 27: 1153–1167. www.doi.org/10.1046/j.1365-2699.2000.00489.x

Yudha DS, Prabowo MA, Suriyanto RA & Barianto DH (2020) The diversity of ray-finned fishes (Actinopterygii) in Plio-Pleistocene Java. Journal of Tropical Biodiversity and Biotechnology, 5(2): 149–156.